

GEOMORPHOLOGIC CHARACTER OF AN UPPER LEONARDIAN
MASS TRANSPORT DEPOSIT, MIDLAND BASIN:
INSIGHTS FROM 3D SEISMIC DATA

APPROVED BY SUPERVISORY COMMITTEE:

Dr. Sumit Verma, Ph.D.
Chair

Dr. Robert Trentham, Ph.D.

Dr. Mohamed Zobaa, Ph.D.

Ron Bianco, M.S.

Dr. Shawn Watson, Ph.D.
Graduate Faculty Representative

GEOMORPHOLOGIC CHARACTER OF AN UPPER LEONARDIAN
MASS TRANSPORT DEPOSIT, MIDLAND BASIN:
INSIGHTS FROM 3D SEISMIC DATA

By

PARITOSH BHATNAGAR, B.S.

THESIS

Presented to the Graduate Faculty of Geology of

The University of Texas Permian Basin

In partial Fulfillment

Of Requirements

For the Degree of

MASTER OF SCIENCE

THE UNIVERSITY OF TEXAS OF THE PERMIAN BASIN

December 2018

ACKNOWLEDGMENTS

I would like to acknowledge the constructive reviews by my advisor and his constant support to better my knowledge throughout my academic career and to my committee members for their suggestions for this project.

I would like to thank Ron Bianco from Fasken Oil and Ranch for giving the university the C Ranch dataset and giving his invaluable insights to help accomplish this research.

I would like to thank Troy Tittlemier from Trey Resources for his insightful advice and stimulating discussions throughout my research experience and bring clarity to this paper.

I would also like to acknowledge Ron Kenney from EOG Resources for his constructive reviews from which I have greatly benefited.

ABSTRACT

The Permian Basin is a structurally complex sedimentary basin with an extensive history of tectonic deformation. As the basin evolved through time sediments dispersed into the basin floor leading to various mass movements that are well documented in the Permian period. One such mass movement was observed on 3D seismic in the Upper Leonard interval (Lower Permian) of the Midland Basin that is characteristic of a Mass Transport Deposit (MTD). Even though mass movements have been extensively studied within the Permian Basin, little work has been published on the geomorphological expression of MTDs on seismic.

The 350 feet thick MTD mapped in the study area is 5 miles wide in its most chaotic zone, extends up to 14 miles basinward and covers only the translational and compressional regime of the mass movement. The MTD exhibits an array of features (thrust faults, slide/slump and lateral wall) that have been well documented by previous researchers in addition to a unique sedimentary feature, unlike those observed previously that is interpreted as gravity spreading. Internally, the MTD is characterized as chaotic, semi-transparent reflectors terminating laterally against a coherent package of seismic facies interpreted as the lateral wall. The thrust faults within the discontinuous MTD are mapped using geometric attributes such as coherence and structural curvature. Kinematic evidence provided by the upper Spraberry structure suggests the overall MTD flow direction was from the North toward bathyal depths before getting deposited in the medial basin centered

portion of the Midland Basin. Well log analysis shows the MTD as a mix of carbonates and shales with moderate to high resistivity response which are interpreted as slope strata.

TABLE OF CONTENTS

ACKNOWLEDGMENTS	ii
ABSTRACT	iii
LIST OF FIGURES	vii
Chapter 1: INTRODUCTION	1
Chapter 2: GEOLOGIC SETTING	6
2.1 Overview of the Permian Basin	6
2.2 Geologic Setting of the Leonardian Series	8
2.3 Previous MTD Studies	11
Chapter 3: METHODS	14
Chapter 4: MASS TRANSPORT DEPOSITS CLASSIFICATION, PROCESSES AND MORPHOLOGY	16
4.1 Classification	19
4.2 Processes	19
4.2.1 Slides	21
4.2.2 Slumps	21
4.3 Staging Area for Mass transport deposits	22
4.4 External and Internal Morphology	23
Chapter 5: CHARACTERIZATION OF A MASS TRANSPORT DEPOSIT USING SEISMIC ATTRIBUTES	27
5.1 Sobel Filter (Coherence)	27
5.2 Structural Curvature	32
5.3 Seismic Amplitude	37
5.4 Lithologic Character of the MTD in the Midland Basin	39

Chapter 6: DISCUSSION AND CONCLUSIONS	43
REFERENCES	46

LIST OF FIGURES

Figure 1: Paleogeography of Permian Basin in early Permian time showing study area in the red box

Figure 2: Interpreted regional 2D line trending NW-SE illustrating the prograding carbonate platform basinward due to forced regression

Figure 3: A simplified stratigraphic chart correlating shelf to basin facies (modified from Handford, 1981). The red box indicates the stratigraphic interval in which the MTD was deposited

Figure 4: Isopach map of the Upper Spraberry interval. Arrows indicate the primary sediment flow into the basin during time of deposition (redrawn from Handford 1981a). Study area within red box

Figure 5: Different process responsible for mass-transport deposits (modified from Festa et al., 2016). Blocky flow deposits represent a transitional zone between slump and debris flow deposits

Figure 6: The different processes comprising of a MTD and turbidity flow (modified and redrawn from Posamentier et al., 2010)

Figure 7: a) A small MTD observed in the Austrain Alps; b) Compression and extension associated with mass transport deposit. Modified after Posamentier (2017)

Figure 8: **A)** seismic cross section XX', **B)** coherency slice, **C)** interpreted line diagram showing the steeply dipping flanks. The big arrow indicates the direction of sediment flow (modified after Posamentier and Martinsen, 2010)

Figure 9: Section view characterizing the chaotic internal reflectors of the MTD in the Delaware Basin (modified after Allen, 2013)

Figure 10: Coherence extracted on a stratal slice showing thrust faults (dipping NW), lateral wall and overall sediment direction.

Figure 11: NW-SE seismic cross section showing internal reflector configuration of the MTD and interpreted line diagram

Figure 12: W-E seismic cross section showing internal reflector configuration of the MTD and interpreted line diagram

Figure 13: NW-SE cross section illustrating how coherence, k_1 and k_2 anomalies are mapped on the thrust faults

Figure 14: a) co-rendered image of coherence with k_2 anomaly; b) co-rendered image of coherence with k_1 anomaly; c) co-rendered image of coherence with k_1 and k_2 anomaly. Notice the localized k_2 anomaly behind the compressional event

Figure 15: Top of MTD surface co-rendered with coherence and k_2 anomalies highlighting the thrust faults and “v” shaped scour marks. Overall sediment direction is interpreted to be coming in from the North

Figure 16: Seismic amplitude values extracted on stratal slice showing the change in amplitude anomalies going up the MTD stratigraphic section (left to right). The overall geometry of the MTD is hard to discern using amplitude values by itself

Figure 17: Well logs indicating MTD as a mix of carbonates and siliciclastic sediments

Figure 18: Overall interpretation of the Upper Leonard MTD observed in the Midland basin

CHAPTER I

INTRODUCTION

The Leonardian Series of the structurally complex Permian basin had shelf to open marine depositional environment with many sedimentary features. In the Midland Basin of West Texas, the Leonard Series (Lower Permian) include siliciclastic and carbonate rocks that were deposited in deep-water marine environments with detrital limestone restricted to slope and base of slope settings (Hamlin et al., 2013). Previous studies show the sediments were deposited as a large basin-floor submarine fan system and are commonly interpreted as deposits of turbidity currents and debris flow (Handford, 1981). A different spectrum of mass movement was observed on 3D seismic within the Upper Leonardian interval of the Midland Basin which are representative of mass transport deposits (MTDs). In this study a MTD is described as a gravity flow deposit in which grains remain intact with respect to one another as opposed to turbidity deposits. The MTD mapped in this study covers parts of Andrews, Ector, Midland and Martin counties in the Midland Basin (Figure 1) and is in the vicinity of the Spraberry trend which accounts for one of the largest plays in the world both conventionally and unconventionally (Bhatnagar et al., 2018) .

Mass movements generate the most impressive deposits in terms of volume on the Earth's surface, in both subaqueous and subaerial settings. Nissen et al. (1999) were the first one to document the various aspects of mass movements in seismic data using coherence attribute in the Nigerian continental slope including MTDs. Such sedimentary deposits are distinctive in deepwater depositional systems mostly due to their large size,

geomorphology and chaotic internal character (Shipp et al., 2011). These deposits along with the process that creates them can have significant hazards by triggering tsunamis or destabilizing drilling platforms and seafloor petroleum collection (Martinez, 2010). However, MTDs can play a significant role in petroleum exploration as they may be top and lateral seals, or may have acted as paleobathymetric constraints on deposition of overlying reservoir deposits (Amerman, 2009). MTDs are in essence Earth's modern and ancient deepwater stratigraphic record and are an important tool in our understanding of mass movements in slope settings.

With the recent advent of 3D seismic technology and its remarkable spatial resolving power, MTDs are better defined with their full areal extent and their morphologic features in areas affected by slope failure. Posamentier gives us a detailed overview of MTDs in terms of emplacement processes, depositional products, and their stratigraphic distribution with insights from outcrop and 3D seismic data (Posamentier, 2010). It should be recognized that it is imperative to integrate borehole data along with seismic section and plan view to properly define MTDs and understand their lithological character for reservoir potential (Davies et al., 2007).

Allen et al. (2013) studied MTDs in the Bone Springs formation in the Delaware Basin of West Texas, USA in which the authors utilized seismic and well log data to map the compressional feature of the MTDs along with the log responses to highlight the MTDs reservoir potential. In another study, Asmus et al. (2013) investigated the architectural attributes of less than 3 feet thick turbidites and MTDs in the Delaware basin and concluded that more than 90% of these deposits are easily identified in image logs with decreasing

gamma ray and increasing resistivity responses. Amerman (2009) explored the structure and stratigraphy of deepwater MTDs in the Permian Cutoff Formation and overlying Brushy Canyon Formation in the Delaware basin to analyze the internal architecture and stratigraphic relationship of MTDs in successions. Much like the studies conducted in the Delaware Basin from outcrop, image and wireline logs, correlations will be inferred to help map the MTD in the Midland Basin and understand its geomorphologic expression with the help of seismic data.

Even though mass movements have been well documented in the lower Permian period, prior to this study, no other author had reported or studied the MTDs in the Upper Leonard interval of the Midland basin with the help of seismic data. The following study aims to identify and characterize the MTD observed in the medial basin-centered portion of the Midland Basin. The MTD is visualized through 3D seismic data along with seismic attributes to delineate the shape, size and anatomy of this sub-surface feature. The objective is to integrate well logs and seismic data along with paleobathymetry to better understand the geologic evolution of the MTD.

The thesis is divided as follows: Chapter II discusses the evolution of the Permian Basin through time and sets the geological background of the study area with a focus on the Lenoarndian series. It further discusses the different structural elements present in the Midland Basin and their effect on subsequent sediment influx into the study area during the Upper Leonard interval.

Chapter III talks about the methodology and discusses the available 3D seismic and well log data along with geometric attributes such as Sobel Filter (coherence) and Structural Curvature that are used in this study to highlight the discontinuous features observed within the MTD.

Chapter IV forms the basis for MTD classification, different processes that comprises an MTD and their internal and external morphologic expression. It further gives the readers an insight of what an MTD looks like in seismic by looking at an example from offshore Gulf of Mexico and one compressional event from the Delaware Basin.

Chapter V delineates the MTD mapped in the study area and ties in with geology to interpret the overall sediment direction. Seismic attributes are utilized to understand the shape and size of the MTD and interpret different sedimentary phenomenon. Wireline logs are analyzed within the MTD interval to understand the sedimentary features lithologic character and possible reservoir potential.

Chapter VI discusses the results presented in this study and concludes with an overall interpretation of the MTD mapped in the study area.

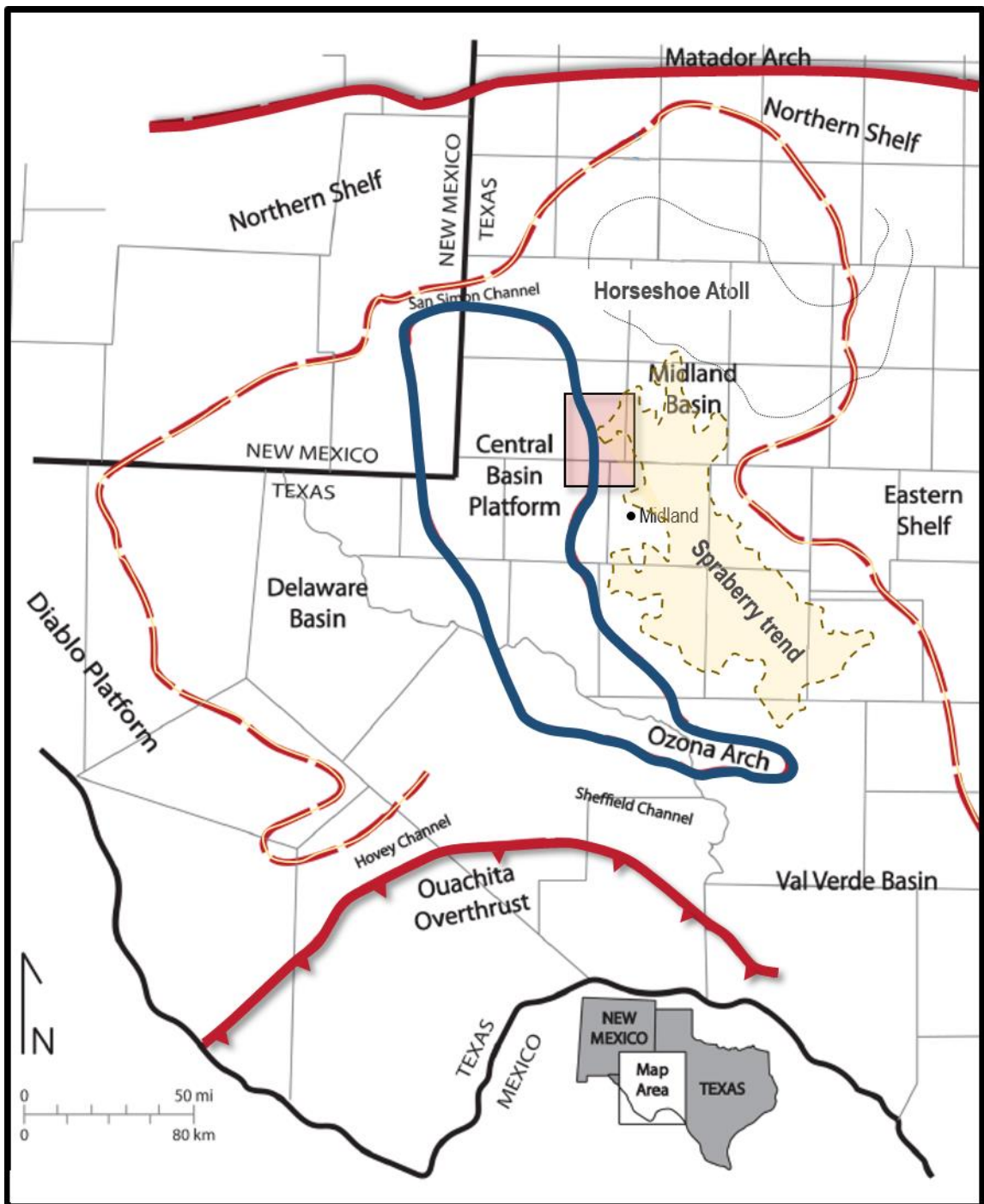


Figure 1: Paleogeography of Permian Basin in early Permian time showing study area in the red box (modified from Ruppel, 2000).

CHAPTER II

GEOLOGIC BACKGROUND

Overview of the Permian Basin

The Permian Basin is a structurally complex sedimentary basin with an extensive history of tectonic deformation. The extent of the Permian Basin spans an area of approximately 250 miles wide and 300 miles long in West Texas and Southeastern New Mexico of the United States. The sedimentary section of the Permian Basin comprises of Paleozoic carbonates on the shelf while siliciclastic and some carbonates accumulated on the slope and within the basinal regions. Stratigraphic correlations of abrupt changes in facies type between the platforms and the basin floor can be challenging, although this has been well documented (Ruppel et al., 2000; Playton et al., 2002). Study of sequence stratigraphy from shelf to basin sediments using modern seismic surveys with good vertical and horizontal resolution allows us to better understand the basin's complexity. With an integrated approach using wire-line and seismic data, relative ages of major sedimentary features can be mapped and studied. This thesis focuses on visualizing and describing a MTD that was deposited in the Midland Basin, in the Upper Leonardian, which is in the Permian period.

The Permian Basin is known for its unconventional shale plays and at present has reached a production of 2.8 million barrels per day (BPD), making it the world's second largest energy producer behind Ghawar in Saudi Arabia (Rapier, 2018). During Cambrian through Mississippian, before the Permian Basin completely formed, it was first described

to be a shallow marine, slightly dipping basin referred to as the Tobosa Basin (Hoak, 1998). Sedimentation was relatively uniform and consisted of widespread shelf carbonates and thin basinal shales (Hills, 1983). Tectonics were fairly subtle up until the collision phase in the Late Mississippian – Early Pennsylvanian when North America plate rifted and collided with the South America and African plate giving rise to the Marathon - Ouachita Orogeny. This compressional event deformed the Tobosa basin that uplifted the basement block along pre-existing zones of weakness giving rise to rapid subsidence and sedimentary filling. By later Paleozoic time, the Tobosa basin was divided into two major basins: Delaware Basin (to the west) and the Midland Basin (to the east) separated by the NW trending Central Basin Platform (uplifted basement block). The Midland basin, which is our study area, is a deep water basin bounded by carbonate platforms which originated during pre-Permian uplift: Central Basin Platform, Northern Shelf, Horseshoe Atoll (an isolated platform in the North) and the Eastern Shelf (Hamlin et al., 2013).

Tectonism was greatest during the Early Pennsylvanian but persisted into the Early Permian (Wolfcampian) (Ross, 1986). By the beginning of the Leonardian, however, tectonic uplifts had become depositional platforms, preferred sites for carbonate buildups. The Horseshoe Atoll, an isolated carbonate platform in the northern Midland Basin began in the Pennsylvanian as a broad carbonate buildup that was surrounded by basinal environments (Vest, 1970). By the Early Permian, more than 1,000 ft of relief had developed on the aggrading platform system. Starting in the Wolfcampian and continuing through the Leonardian, the Horseshoe Atoll was buried by deep-water siliciclastic sediments (Vest, 1970). However, differential compaction of sediment overlying the peak-

and-saddle morphology of the Horseshoe Atoll influenced the sedimentation patterns of the upper Spraberry formation (Upper Leonardian). The structural morphology of the upper Spraberry formation and how the sediments were coming into the basin forms the basis for our understanding of the MTD deposition.

Geologic Setting of the Leonardian Series

The Leonardian stratigraphy in the Midland Basin records deposition in an intracratonic deep water basin, bounded by shallow water carbonate platforms (Hamlin et al., 2013). Sea level fluctuations controlled sediment input into the basin by flooding or exposing the platform. Slope environments, which separate the basin floor from surrounding shallow-water platforms, are characterized by abrupt stratigraphic discontinuities, detrital carbonates, and clinoform geometries (Hamlin et al., 2013). This is evident in Figure 2 which shows a regional 2D line trending NW-SE from the Northern shelf into the Midland basin illustrating the prograding carbonate platform (clinoformal geometries) basinward.

The Upper Leonardian interval which conforms on top of the Spraberry formation is equivalent to Glorieta formation (Figure 3) on the platforms (Handford, 1981b). Understanding the palaeobathymetry of the underlying Spraberry formation with the help of isopach and regional cross sections can provide useful information on how the sediments were dispersed to the basin floor and how the underlying seabed exerted control on the morphology of the overlying MTD.

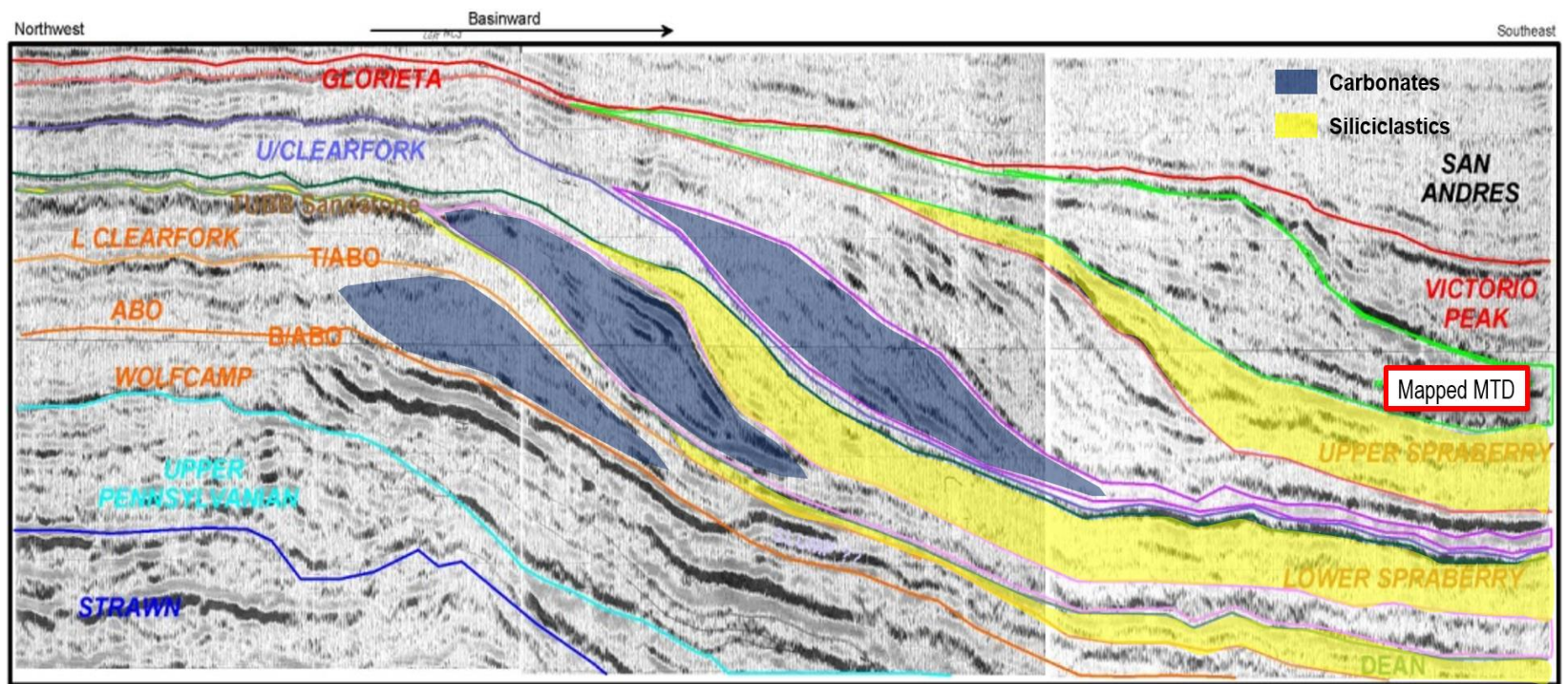


Figure 2: Interpreted regional 2D line trending NW-SE illustrating the prograding carbonate platform basinward due to forced regression (modified and used with permission after Trentham, 2018).

The Spraberry formation of the Midland Basin is a major oil producing formation from heterogeneous submarine fan reservoirs (Tyler et al., 1997). Regional mapping of the 1,000 ft thick Spraberry fan cone shows that the fan system was deposited in water depths of 600 - 1,000 ft (Handford, 1981b). The Spraberry can be delineated by three sand bodies in the upper Spraberry and four in the lower Spraberry separated by 250 ft of limestone. (Tyler et al., 1997). This cyclic repetition of terrigenous clastics and carbonates and shales identifies primarily carbonate or clasticly dominated shelf. Most sedimentologic evidence

STRATIGRAPHIC CHART			
System	Series	Central Basin Platform	Midland Basin
PERMIAN	GUADALUPIAN	TANSILL	TANSILL
		YATES	YATES
		7 RIVERS	7 RIVERS
		QUEEN	QUEEN
		GRAYBURG	GRAYBURG
		SAN ANDRES	SAN ANDRES
	LEONARDIAN	GLORIETA	U. LEONARD
		U. CLEARFORK	U. SPRABERRY
			L. SPRABERRY
		TUBB	DEAN
		L. CLEARFORK	L. CLEARFORK
	WOLFCAMP	WOLFCAMP	WOLFCAMP

Figure 3: A simplified stratigraphic chart correlating shelf to basin facies (modified from Handford, 1981). The red box indicates the stratigraphic interval in which the MTD was deposited.

suggest that these terrigenous clastics were deposited by density current deposits as opposed to turbidity currents.

Basin wide maps of sandstone distribution in the broadly defined lower and upper Spraberry clastic members (Handford, 1981 a, b) show that the principal sediment sources lay to the northwest, north, and northeast. This is evident in the Upper Spraberry isopach map which shows depocenters around the Horseshoe Atoll in the north indicating probable entry points (Figure 4). The toe of shelf slope also influenced paths of sediment transport, particularly for sediment entering the basin from the principal northwest sediment entry point. Wireline correlations (Ruppel et al., 2000) indicate that cyclic Leonardian platform deposits started prograding towards the basin into massive, clinoformal carbonates on the slope, which in turn, grade into flat lying calcareous and siliciclastic intervals.

Previous MTD Studies

In the Midland Basin, Wolfcampian (Early Permian) interval have been known to host mass movements from the platforms where calcareous highstand intervals, which form equally widespread layers on the basin floor, are composed of hemipelagic deposits (mudrocks and calcareous mudrocks) and detrital carbonate mass-transport deposits (Hamlin and Bomgardner, 2013). Leonardian sequence stratigraphic interpretations in Midland Basin are based on studies of outcrops along the western margin of the Delaware Basin by Fitchen and others (1995), Kerans and others (2000), and Ruppel and others (2000).

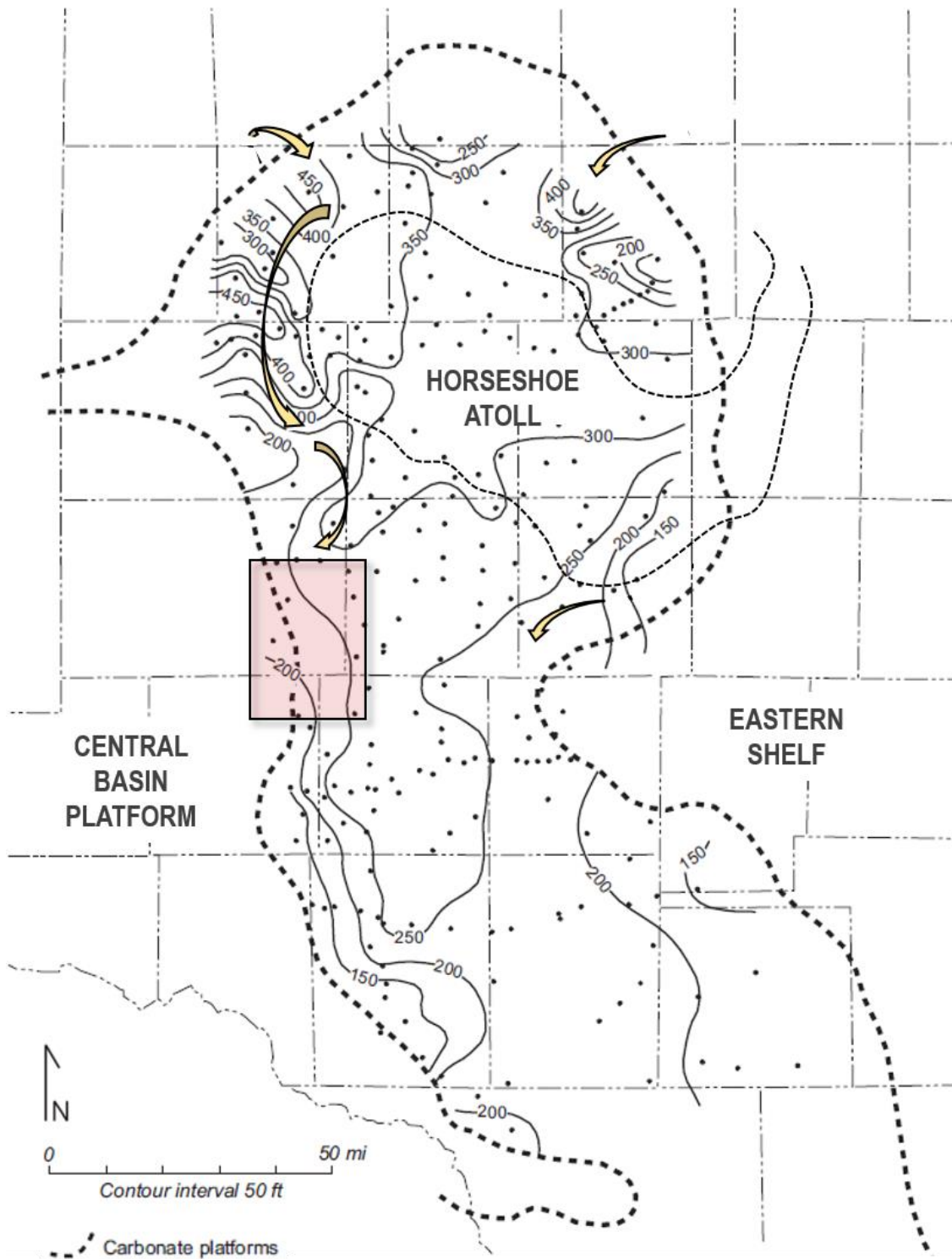


Figure 4: Isopach map of the Upper Spraberry interval. Arrows indicate the primary sediment flow into the basin during time of deposition (redrawn from Handford 1981a). Study area within red box

Asmus (2013) talks about the characterization of deepwater carbonate turbidites and mass transport deposits using borehole image logs in the Upper Bone Spring formation (Upper Leonardian) of Delaware Basin, Southeast New Mexico and West Texas. The study investigates the architectural attributes of less than 3 feet thick turbidites and MTDs and concludes that more than 90% of these deposits are easily identified in image logs. Increasing deformation of deposits towards the central portion is correlated to high and low resistivity bedding layers observed in whole core and image logs. The following correlations will be used to help characterize the MTD in our study area.

Overlying the Bone Spring is the Permian Cutoff formation (Upper Leonardian) and Brushy Canyon formation (Guadalupian) in the Delaware Basin of West Texas. This outcrop study conducted by Ammerman (2009) comprises of a relatively fine-grained (mostly mud-medium sand) carbonate-siliciclastic depositional system that experienced little to no syndepositional tectonism. The significance of the study was to study the soft sediment deformation of the MTD and infer the paleobathymetry of the top of Cutoff formation and its control on overlying deepwater sedimentation patterns. Much like this study, we analyzed the paleobathymetry of the upper Spraberry formation (tectonically inactive) of the Midland Basin to understand the MTD sedimentation pattern.

Mass movements have been extensively studied within the Permian Basin, however little work has been published on the nature of these MTDs and their related geomorphological expression on seismic. The following sections describes the many processes that leads up to a MTD and how to classify the different components of MTDs through seismic signature.

CHAPTER III

METHODS

The C Ranch 3D pre-stack time migrated (PSTM) mega merged seismic data was donated by Fasken Oil and Ranch and covers parts of Andrews, Ector, Midland and Martin County with a seismic outline of approximately 440 square miles (Figure 1). All the seismic surveys were acquired with Vibroseis with a sweep of 8-90 Hz, a 2 ms sample rate and processed with a bin size of 110 feet x 110 feet. The seismic data presented in this study follows SEG polarity where increase in impedance is a peak (positive amplitude) and a decrease in impedance is a trough (negative amplitude).

Assuming the limit of seismic resolution is one-fourth of a wavelength, the limit of vertical resolution (h) for the MTD within the upper Leonard interval was determined using a central peak central frequency (f) of 32 Hz, an interval thickness (Δx) of 350 ft (107 m) and a one-way travel time of (t) 0.025 seconds.

$$\textit{Vertical resolution } (h) = \frac{1}{4} ((\Delta x / t) / (f)) = 109 \text{ ft (33 m)}$$

The MTD mapped in the study area represents an amalgamated flow with vertical stacking of sediments which exceeds the minimum thickness of the vertical resolution, making it possible to be observed in seismic. Their seismic signature is characterized by discontinuous seismic reflectors represented by a series of thrust faults. The MTD mapped in the study area covers only the translational and compressional regime of the mass movement.

Well Fasken David BR was used to tie in the well tops with the seismic and establish a time to depth relationship. A continuous seismic reflector within the upper Leonard interval was picked with high level of confidence across the entire survey. The picked horizon was flattened and the MTD was mapped with the help seismic attributes using stratal slices. Geometric attributes such as Sobel filter (a type of coherence) and Structural curvature were computed on the MTD interval using AASPI software. The resultant attributes were brought into Petrel and studied using stratal slices.

Sobel filter is a very famous sharpening algorithm commonly used in Photoshop and image-processing software. The way this filter is implemented in seismic is by mapping trace by trace discontinuity based on waveform and amplitude changes along the structural dip of inline and crossline directions (Luo et al., 1996). Structural curvature on the other hand is the derivative of dip along the inline and crossline direction which maps the curvedness of a surface. Curvature attributes are usually associated with faults or folds and measure the strain of the rock which could be correlated to fractures. Incorporating both the attributes helps define the overall geometry of the MTD and bracket the fault trace within the compressional event.

Additionally, wireline logs were used to understand the MTDs lithologic character. The wells logs were selected on the basis of log quality, resolution and depth of penetration in the area of interest. Conventional wireline logs utilized for this study include gamma ray, caliper log, shallow and deep resistivity, neutron porosity and density porosity logs. The top and base of the MTD was picked on a low gamma ray/high resistivity log response.

CHAPTER IV

MASS TRANSPORT DEPOSITS CLASSIFICATION, PROCESSES AND MORPHOLOGY

Mass movements represent the main mechanism of sediment transport in deep water settings and can range from meter to several miles in dimension. Depending on the type, mass movements can range from turbidites (in the form of channels, lobes and in overbank) that are sand prone to Mass Transport Deposits (MTDs), contour-current deposits and pelagic and hemipelagic (drape deposits) that are mud prone (Posamentier and Martinsen, 2010). These gravity flow deposits can be divided into two main categories: Mass transport and Turbidite Deposits. The term MTD include only those processes where sediments are moved *en masse* (i.e., grains don not move freely with respect to others). In mass-transport processes, the main grain support mechanism is not fluid turbulence. Thus, turbidity currents are excluded (Asmus, 2013). Even though MTDs are considered separate from turbidites, it should be recognized that a single depositional event can generate both types of deposits as they are part of the same depositional process.

Posamentier (2017) points out that one can determine if you are in a deep water setting from seismic data by looking for the presence of widespread polygonal faulting (i.e., shrinkage cracks), sediment waves, seismically resolvable MTDs and presence of clinofolds defining deep water setting (geomorphology). On seismic, MTDs have characteristic stratigraphic and geomorphologic features: basal linear grooved and scoured surfaces, hummocky relief at the top, and chaotic seismic facies, with internal thrust

faulting common (Posamentier and Martinsen, 2010). The term MTD encompasses several slope deformational processes, including creep, slide, slump and debris flow (Jenner et al., 2007). The slide/slump stage will be discussed later in this study as it comprises the MTD mapped in the Midland Basin.

The entire spectrum of a mass movement from slide/slump to turbidity flow is termed as an Olistostrome (Figure 5). The working hypothesis for the type of flow depicted in figure 5 is that relative sea level changes influence equilibrium conditions on upper slope changing pressure/temperature conditions and potential dissociation of gas hydrates. This leads to slope instability/failure and resulting MTD deposition. Some of the common triggering mechanism influencing slope instability include re-activation of pre-existing extensional faults, fluctuations in sea level and dissociation of gas-hydrates (A. Festa et al, 2016). The type of deposit (creep, slide and slump or debris flow) to be expected depends on the slope gradient, resulting sediment velocity and the hydrostatic forces between the sediment and fluids. Slope failures caused by gas hydrates and subsequent MTD deposition are most common in offshore settings.

Previous studies done in the Delaware Basin of the Bone Spring Formation (Upper Leonardian) suggest that shelf edge and slope deposition of sediments occurred as a result of decreased accommodation space due to increased carbonate production and hydraulic degradation and over-steeping of a vertically aggrading shelf margin, among others. (Gawloski, 1987; Saller et al., 1989; Wiggins and Harris, 1985).

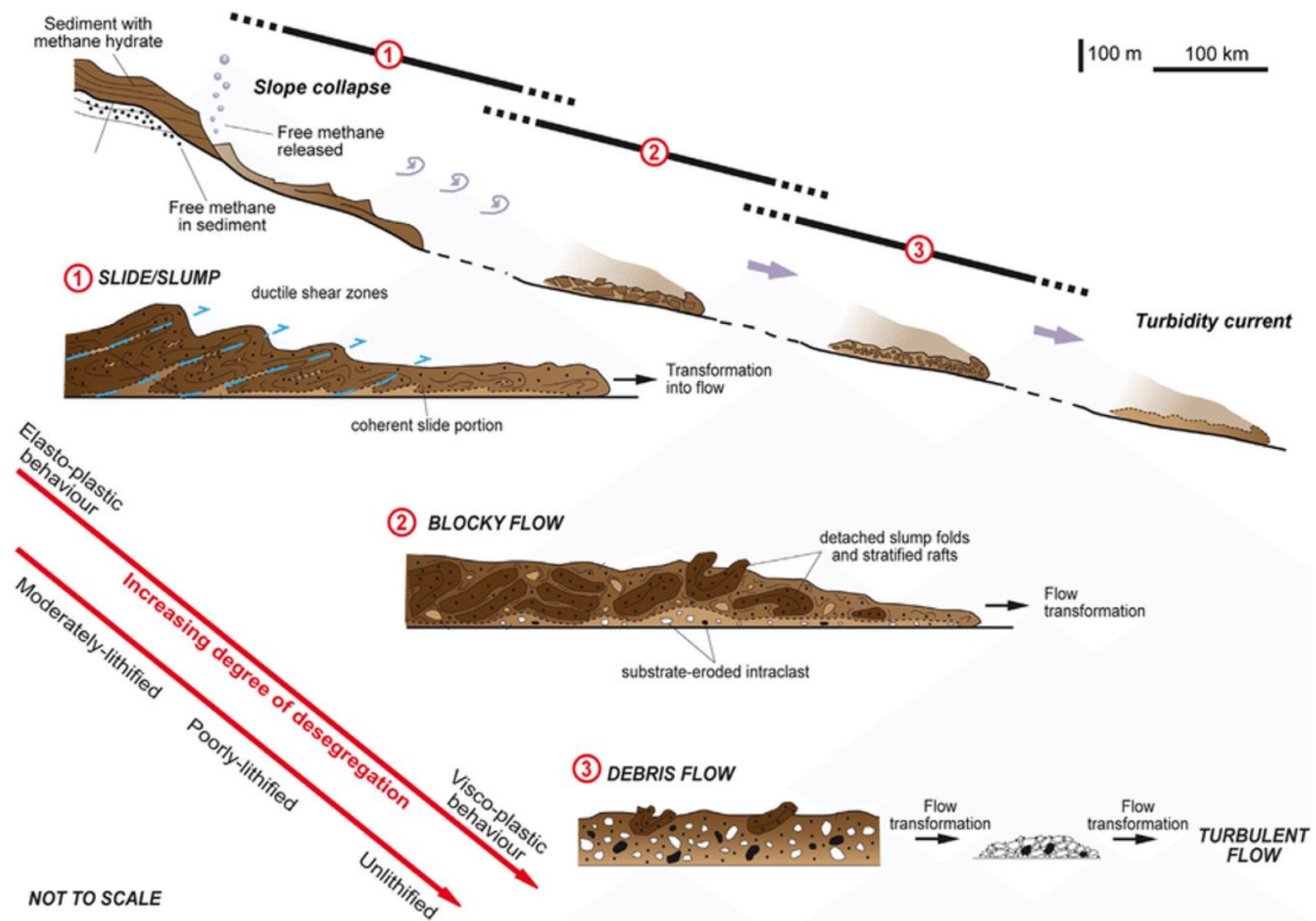


Figure 5: Different process responsible for mass-transport deposits (modified from Festa et al., 2016). Blocky flow deposits represent a transitional zone between slump and debris flow deposits.

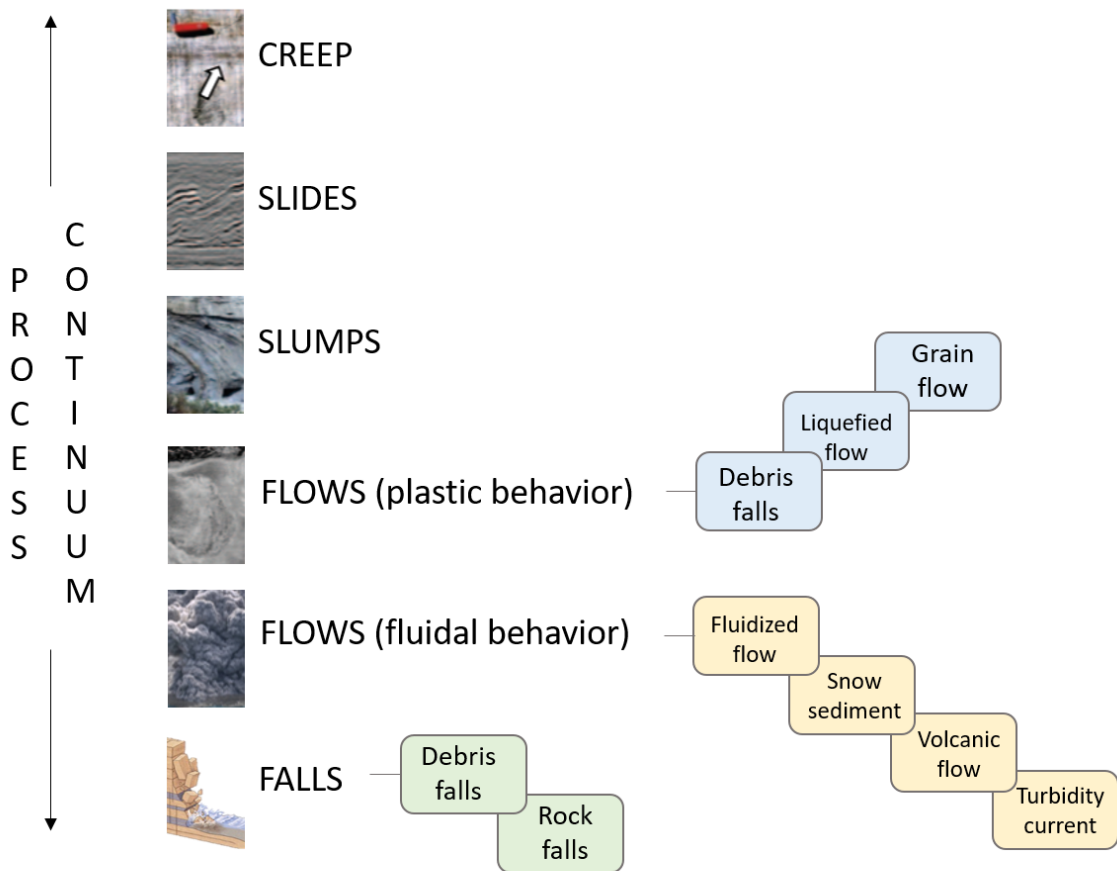
Classification

Mass movement processes can be classified on the basis of climate, type of material moved, and triggering mechanism. Many of these classification schemes do not include subaerial slope failures such as slides and slumps as they are based on subaqueous gravity flows (Martinsen, 1994). This classification scheme was simplified by Nemec (1991), who grouped the processes into six categories accounting for both subaqueous and subaerial processes (Figure 6). It shows a range of mass movements from slow frictional sliding with no relative movement of grains (creep) to increasingly turbulent movement of grains (debris flow). One can also think of this as a continuum process where one process may evolve into another with time, or one depositional process may trigger the other. This scheme is observable at outcrop and at seismic scale. Outcrop expressions are great for studying such features for stratigraphic, lithologic and kinematic details, while 3D seismic provides paleogeographic settings and overall stratigraphic architecture and morphological expression (Posamentier and Martinsen, 2010).

Processes

Slopes are inherently unstable, whether subaerial or subaqueous, as sediments deposited on them are subject to gravitational forces along an inclined surface. Analysis of 3D seismic data allows a full spatial view of MTDs. The principal sediment direction can be easily discerned from such data, although within the MTD the direction of sediment movement can vary due to localized internal kinematics (Prior and Coleman, 1979; Lewis,

1971; Martinsen, 1989). In the following sections, the most common processes that comprise the MTD observed in our study area are discussed.



Redrawn and adapted from Nemeč, 1991, and Martinsen, 1994

Figure 6: The different processes comprising of a MTD and turbidity flow (modified and redrawn from Posamentier et al., 2010).

1. Slides

Slides involve movement of sediments with little to no internal deformation and exhibits a laminar flow throughout the body of the sediment. This is accompanied by translation and/or folding of the sediments as they experience shear failure along a basal deformed zone (Moscardelli and Wood, 2008; Amerman, 2009). In map view, the upslope region is concave downslope and exhibits extensional faulting. The middle region is mainly transitional and most likely not deformed. The terminus or toe region is usually dominated by compressional deformation that produce thrust faults (Martisen and Bakken, 1990; Posamentier and Walker, 2006) and has a series of convex downslope and characteristically lobate forms. This is supported by Butler et al's (2006) recognition that submarine mass transport complexes on the modern sea floor often display complex rugosity on their upper surfaces along with detached faults and folds.

2. Slumps

Slumps are characterized by significant internal deformation leading to imbricate zone geometries (Lewis, 1971; Dingle, 1977) and are usually associated with the toe of slope region. As the sediments approach the lower slope, frictional drag takes over and decelerates the sediment flow causing the sediments to pile up on top of each other that represents a series of low angle thrust faults. Slumping is a common process where there is significant involvement of clay-size sediments (Posamentier et al., 2010). The main fold type observed in a slump are sheath folds formed by simple shear and experiences a main

phase of plastic/ductile deformation where folds are formed, followed by a late brittle phase when faults form (Martinsen, 1994).

The mass movement spectrum between slides and slumps is continuous and hard to distinguish among themselves because an MTD may show characteristic of all two modes of transport (Bakken, 1987). Observations made from previous work (Posamentier 2010; Allen 2013) has been used to help define objectives for this thesis in regards to compartmentalizing the MTD and how to best determine the size, shape and anatomy of the sedimentary feature. Using seismic cross sections, inferring features related to sliding or slumping can be achieved.

Staging area for Mass-Transport Deposits

As the name suggests, this is the area where MTDs originate. The staging area in an unstable slope can arise from a range of factors: (1) sudden movement of sea floor due to seismic events (Seed, 1968; Leeder, 1987); (2) lowering of wave base in response to relative sea level fall, leading to disequilibrium conditions at the seafloor; (3) oversteeping of slopes as a result of fault movement; (4) overpressure associated with fluid expansion and/or mud volcanism; and (5) dissociation of clathrates (essentially gas hydrates) in the near-subsurface section leading to slope failure (Carpenter, 1987; Maslin et al., 1998).

The largest mass transport events commonly originate in the mid to upper slope (Posamentier and Martinsen, 2010) and the lithology character of MTDs is ultimately the lithology present in the staging area. Mass-transport that originate at shelf edge or upper slope contains a mix of sand and mud, whereas those that originate in mid slope or beyond

are more likely mud prone (Posamentier and Martinsen, 2010). Based on the core and wireline study conducted in the Bone Spring Formation (Upper Leonardian), Wiggins and Harris (1985) suggest that slump deposits (a process of MTD) in the Delaware Basin represent the re-working of slope strata.

External and Internal Morphology

Posamentier (2017) proposed a model of how a subaerial MTD looks like in a slope setting (Figure 7). Due to slope failure, the sediment block breaks leaving behind a slump scar and causes the sediments to flow down the slope by extensional structures (e.g., normal and listric faults). As the sediments approach the lower slope, frictional drag takes over and decelerates the sediment flow (Posamentier, 2003). As a result, the sediments pile up on top of each other that represents a series of low angle thrust faults.

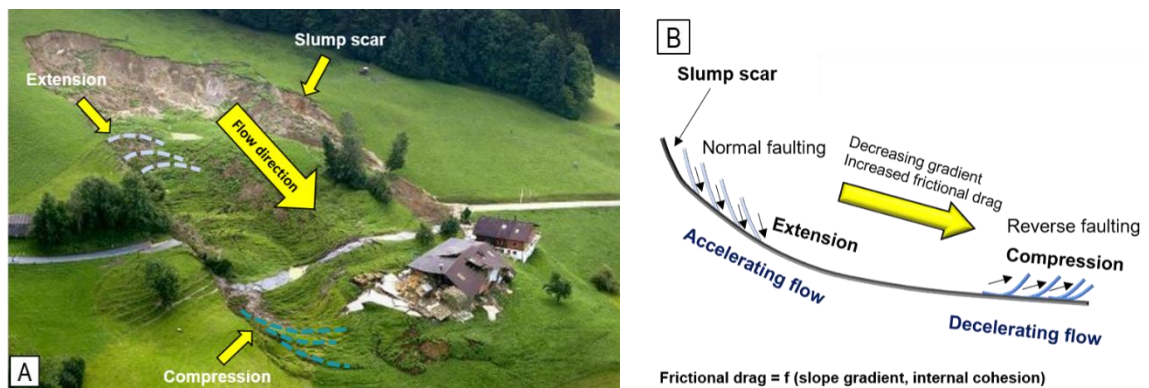


Figure 7: a) A small MTD observed in the Austrian Alps; b) Compression and extension associated with MTD. Modified after Posamentier (2017).

Externally, MTDs can assume a variety of shapes and sizes ranging from lobate to sheet to channel form (Posamentier et al., 2000; Posamentier and Kolla, 2003). The lobes can have steep flanks of up to 20° - 30° suggesting a flow mechanism that involved an abrupt halt and forming low-angle thrust faults as it comes in contact and presses against the terminal wall (Figure 8). The striking linearity of grooves that are commonly observed at the base of MTDs form because of the laminar rather than turbulent flow that characterizes these flows. Sediments close to the terminal wall have presumably travelled the shortest distance (Posamentier and Martinsen, 2010).

Internally, MTDs are described as compressional structures as discussed above. These faults are characterized as listric curvature which originate at the base and extend through the top of the deposit (Figure 8 and 9) orientated parallel to the flow direction (Posamentier and Martinsen, 2010).

In section view MTDs are characterized as transparent to chaotic seismic reflectors (Figure 8a and 9). The following cross section comes from the Bone Spring Formation in the Delaware Basin. The deformed area is characterized by arcuate thrust faults dipping NW (Allen, 2013). The MTD base acts as a detachment surface evidenced by coherent seismic reflector. The overlying strata above the MTD follows similar architecture indicating the MTD is bounded by an interval of approximately 400 feet. The log signature of high and low resistivity response in the deformed MTD zone agrees with the results presented by Asmus (2013).

The internal chaotic nature of MTDs can be sometimes hard to interpret on seismic profiles because of their highly disruptive pattern. To overcome this problem, analysis of seismic profile along with seismic attributes can be the most optimum method to properly characterize the MTD's internal architecture. Knowing the different components that make up an MTD, one can begin to highlight known features with seismic attributes and compartmentalize the sedimentary feature in order to understand the internal anatomy of the MTD in the subsurface. Ultimately, with proper well control and seismic coverage, it is possible to predict potential reservoir targets if any within the MTD system.

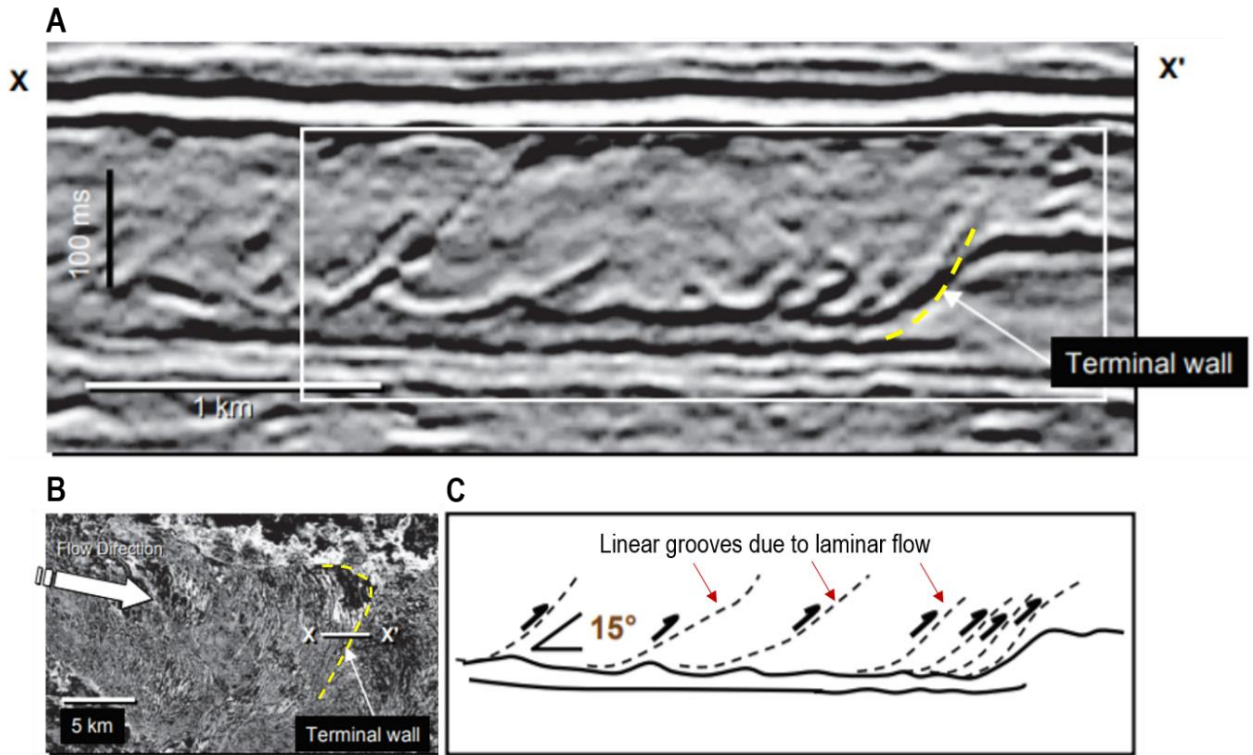


Figure 8: A) seismic cross section XX', B) coherency slice, C) interpreted line diagram showing the steeply dipping flanks. The big arrow indicates the direction of sediment flow (modified after Posamentier and Martinsen, 2010).

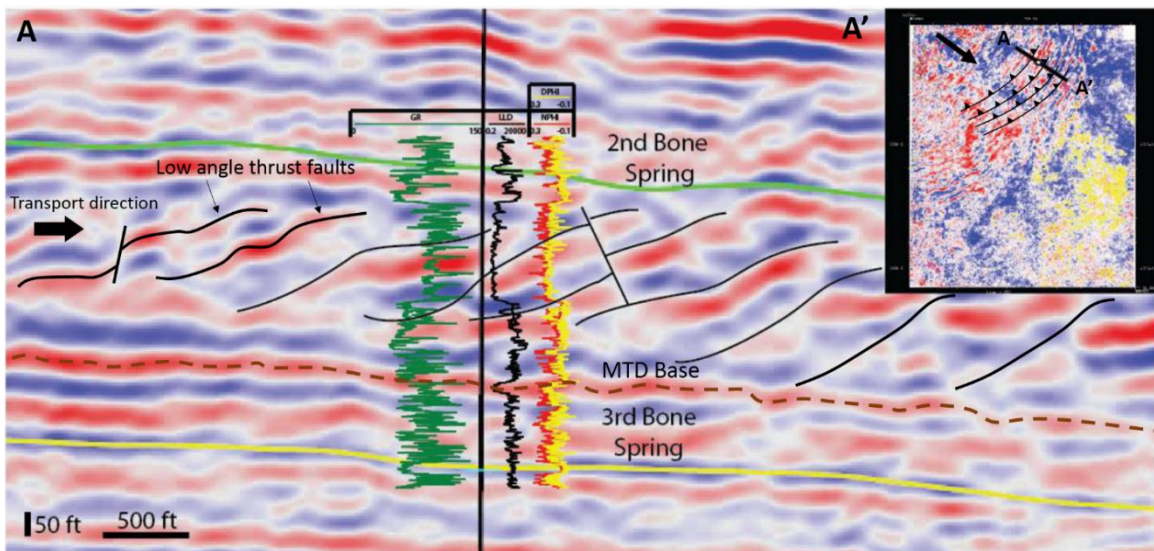


Figure 9: Section view characterizing the chaotic internal reflectors of the MTD observed in the Delaware Basin (modified after Allen, 2013).

CHAPTER V

CHARATERIZATION OF MASS TRANSPORT DEPOSITS USING SEISMIC ATTRIBUTES

3D seismic attributes are quantitative measures or derivative product (Marfurt, 2018) that gives insight on the external and internal geomorphology of geological features. There are several attributes that can be used to map discontinuous features, however geometric attributes are the most useful methodology for studying MTDs (Martinez, 2010). Geometric attributes include coherence, variance, dip, azimuth and curvature amongst others. For this study, coherence and structural curvature attributes were used to help characterize the shape and size of the MTD observed in the Midland Basin and study its internal architecture with the help of seismic profiles. The MTD mapped in the study area covers only the translational and compressional regime of the mass movement; is lobate shape, 5 miles wide and extends up to 15 miles basinward. The following sections discusses how the attributes were used to delineate the MTD.

Sobel Filter (Coherence)

Sobel filter is an edge detection technology that is commonly used in image processing packages that scans the data horizontally and vertically to map discontinuities. That way this filter is implemented in seismic is similar to semblance or variance that is used to map discontinuous features such as channels, faults and fractures (Khoudaiberdiev et al., 2017; Bhatnagar et al., 2017). It detects the break in reflector configuration or lateral

changes in amplitude values and waveform shape (Qi et al., 2017) and provides enhanced image of the small scale geologic feature which helps in understanding the internal complexity of the MTDs. Because of the presence of thrust faults in the toe region, the attribute maps the break in reflector and/or change in amplitude values giving us an overall lobate shape of this sedimentary feature (Figure 10). The following attribute can be used to interpret the internal architecture of the MTD with high level of confidence.

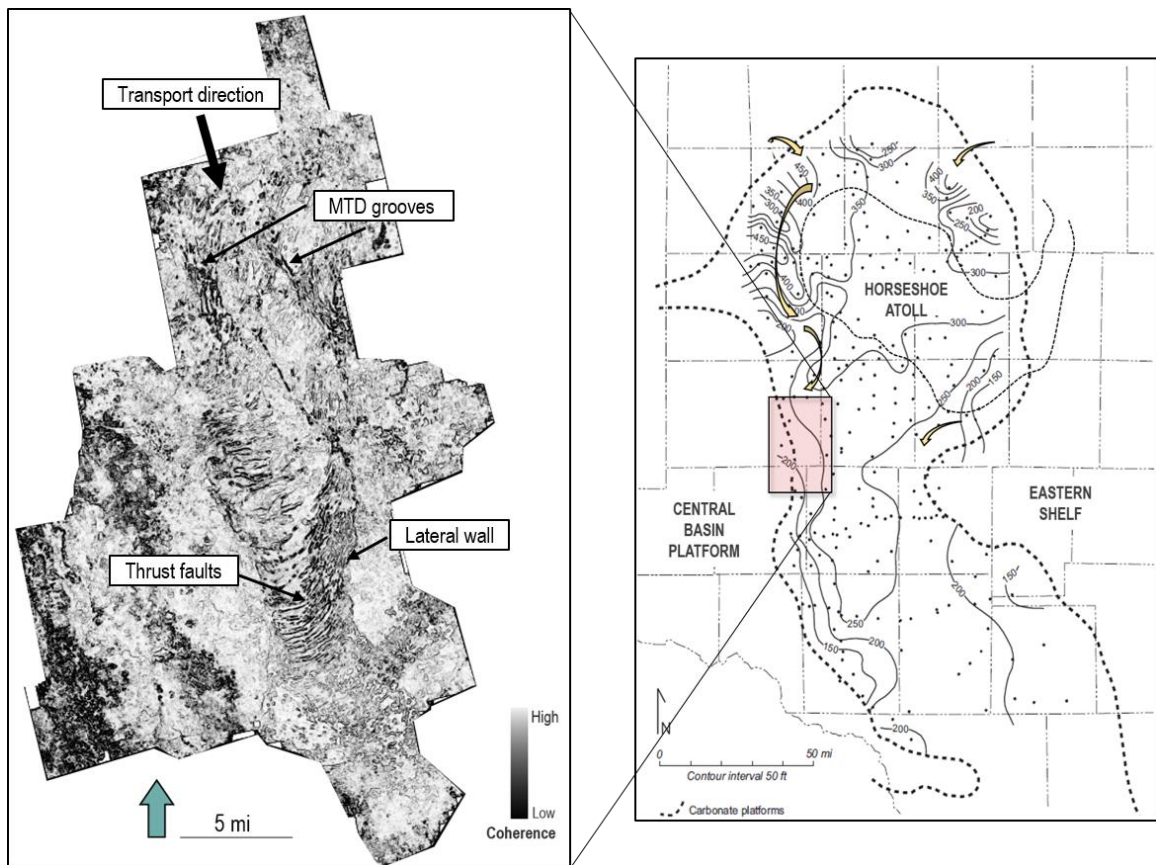


Figure 10: Coherence extracted on a stratal slice showing thrust faults (dipping NW), lateral wall and overall sediment direction.

The discontinuous linear grooves observed within the MTD are thrust faults represented by low coherence values caused by compressional forces as discussed by Posamentier (2010). Since the grooves are oriented in the overall North direction, it is interpreted that the sediments must be coming in from the North (thrust faults align perpendicular to sediment flow). The upper Spraberry isopach map further confirms this regional sediment flow direction. Although within the MTD, the direction of sediment movement can vary due to localized internal kinematics.

The attribute further delineates the presence of lateral wall and the sinusoidal path (interpreted as MTD grooves) the sediments take before settling down. Coherence helps in mapping the discontinuous boundaries of the MTD and give an aerial view of the overall lobate shape of this feature. With the help of seismic section lines, one can begin to start analyzing the slide/slump processes that comprises the MTD.

Slide/Slump

The transverse view (Figure 11) shows a NW-SE trending cross section and gives an insight into the internal architecture of the MTD. Within the MTD, the seismic reflectors seems chaotic and shows the sediments slumping on top of each other forming a duplex structure with a series of imbricate thrust faults. The overall sediment direction is interpreted to be coming from North as the depositional clinoforms (thrust faults) are dipping away from the source. In the SE portion, the reflectors are less chaotic and lacks the abrupt flow of the MTD usually indicated by the presence of the terminal wall. Due to the absence of this terminal wall, it is interpreted that the frontal ramp is buttressed against

a topographic high in the Upper Leonard structure in the SE eventually slowing the sediments down. The seismic further shows continuous reflectors before the compressional event with little to no internal deformation indicating the MTD experienced sliding in this section of the event. The wavy relief observed in the sliding portion shows the compressive nature of these flows with localized faulting and detachment folds.

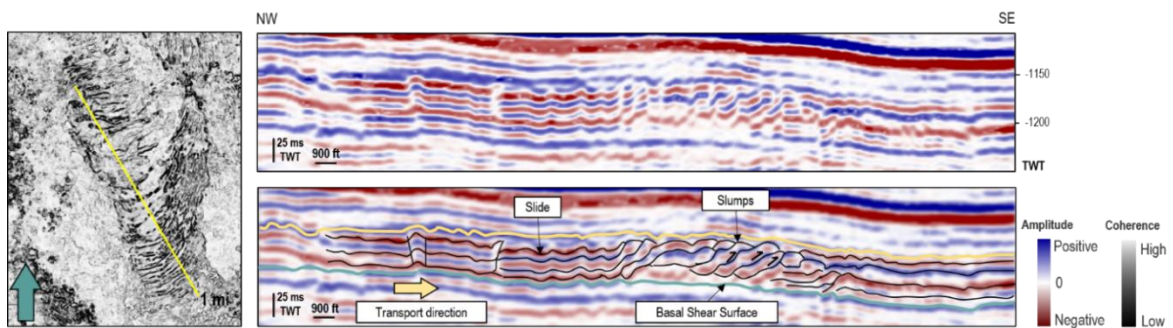


Figure 11: NW-SE seismic cross section showing internal reflector configuration of the MTD and interpreted line diagram

Basal Shear Surface

The entire MTD event overlies the basal shear surface characterized by much more continuous seismic facies (Figure 11). The basal shear zone represents the plane above which downslope translation occurs. In order for mass movements (like MTDs) to be deposited, an underlying surface needs to be present that remains intact and doesn't deform with the sedimentary flow. This surface forms the base of the MTD and makes it possible to see where the first MTD succession occurred on seismic. Depending on the sediment velocity, these flows can sometimes have an erosive nature and can excavate the underlying bathymetry. Identifying the basal shear surface and the top of the MTD reflector (coherent seismic facies; positive amplitude) binds the MTD interval.

Lateral wall

Viewing the reflector configuration from W-E delineates the presence of the lateral wall and its corresponding seismic response (Figure 12). Lateral margins of MTDs are generated parallel to their gross flow direction, and can offer a primary kinematic constraint (Bull et al., 2009). This wall can be identified by an obvious change of going from chaotic to coherent seismic reflectors and helps define the lateral extent of the MTD. They are chiefly associated with strike-slip movements in MTDs (Martinsen and Bakken, 1990). As the sediments translate, they are restricted by the presence of this lateral wall which does not allow the sediments to go past it. As a result, the sediments start shearing in the other direction, eventually slumping on top of each other. On the western margin of the MTD,

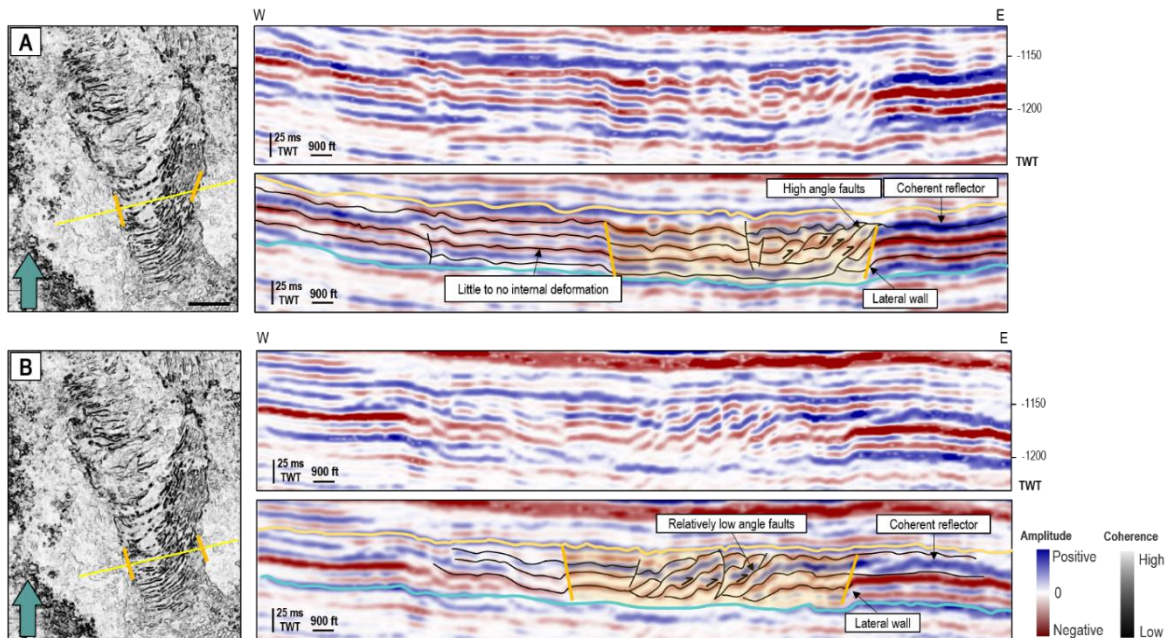


Figure 12: W-E seismic cross section showing internal reflector configuration of the MTD and interpreted line diagram

the underlying bathymetric structure is sloping up towards the Central Basin Platform and the feature is interpreted to stop where the structure begins to climb up.

Another observation to be noted is the orientation of the thrust faults within the MTD that can vary considerably as the thrust faults cut through stratigraphic sections as either ramps or flats. Additionally, repeated slip on other faults and/or associated folding, can cause originally low-angle faults to rotate to steep angles. This is evident in the cross sections (Figure 12) as the thrust faults are dipping at high angles buttressed against the lateral wall where the sediments presumably travelled the shortest distance (Posamentier and Martinsen, 2010).

Structural Curvature

The second attribute used to understand the geometry of the MTD is structural curvature. Structural attributes include the traditional time-structure map, dip azimuth, dip magnitude, and structural curvature among others (Marfurt, 2018). The attribute measures the curvedness of the bending and folding of seismic reflectors by taking the derivative of the dip in the inline and crossline direction. When viewing geologic features in a 3D environment, curvature is subdivided into the most positive principal curvature (k_1) that shows anomaly around the peak of the anticline, and the most negative principal curvature (k_2) that shows anomaly around the trough of the syncline (Verma et al., 2018). One can define different geometric features (bowl, valley, ridge, dome, etc) depending on different k_1 and k_2 values. Additionally, curvature maps the curved deformation adjacent to the faults which helps define the fault traces. Structural curvature was computed to understand the

geometry along with the curved deformation of the MTD. Figure 13 gives a visual of how the algorithm works for a given fault trace to delineate the peaks and troughs of the thrust fault within the MTD. On a plan view, k_2 anomaly (blue colors) indicate valley like feature and k_1 anomaly (red color) represents ridge like feature (Al-Dossary and Marfurt, 2006).

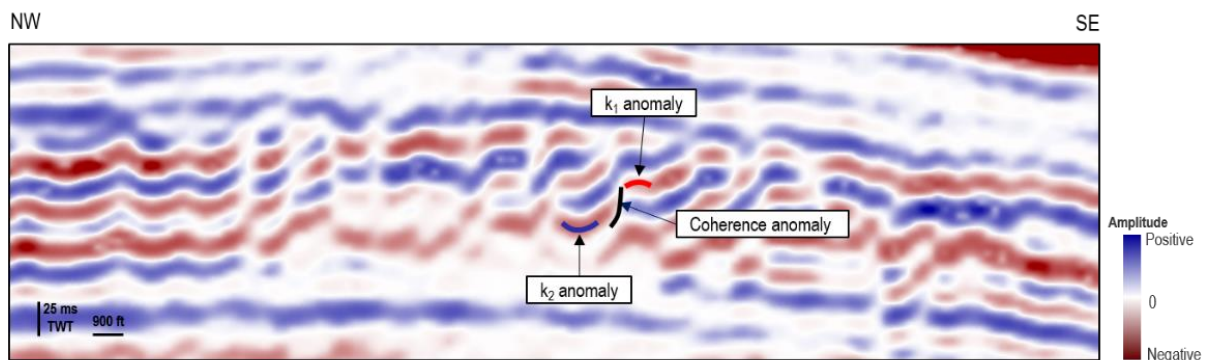


Figure 13: NW-SE cross section illustrating how coherence, k_1 and k_2 anomalies are mapped on the thrust faults.

Figure 14 shows how the anomalies map out once this attribute is applied on the MTD stratal slice. k_2 anomalies highlight the footwall whereas k_1 anomalies highlight the hanging wall of these thrust faults. A unique feature stands out that is coming off from the Central Basin Platform. This curved “arm” feature shows up as a strong k_1 and k_2 anomaly. Although coherence does a great job in delineating the overall shape of the MTD, it fails to highlight this curved geometry that is otherwise picked by the curvature attribute. This anomaly is due to a deep seated Paleozoic fault and over time the sediments conforms on top of this structure resulting in a bend in the stratigraphic section. The curvature attribute is picking this bend in the structure. Coherence does not pick this anomaly because the reflector is continuous and exhibit similar waveform and amplitude values along the dip.

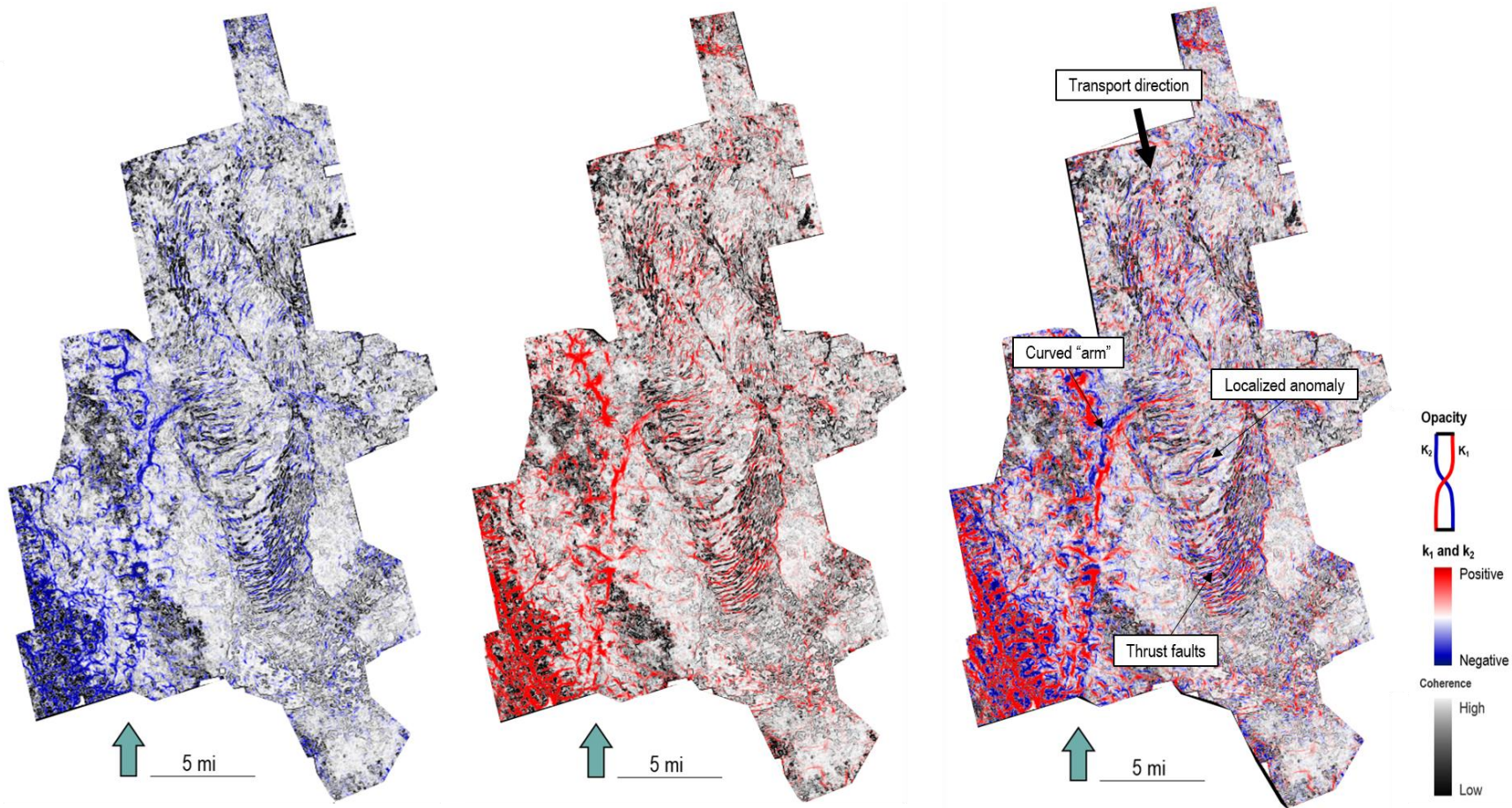


Figure 14: a) co-rendered image of coherence with k_2 anomaly; b) co-rendered image of coherence with k_1 anomaly; c) co-rendered image of coherence with k_1 and k_2 anomaly. Notice the localized k_2 anomaly behind the compressional event

The presence of this curved feature is interpreted to have some influence on the overall kinematics of the sediment flow and the shape of the MTD.

Another anomaly that was picked by the structural attribute and observed within the MTD body are the presence of discontinuous localized events before the compressional regime that is represented by a strong k_2 anomaly (Figure 14c). These peculiar features trend orthogonal to the overall sediment flow and represents a sedimentary flow that is not related to thrust faulting. The phenomenon that is causing this effect is referred to as gravity spreading.

Gravity Spreading

Gravity-driven deformation have been widely documented in salt and ice-related compressional deformation (e.g. Andersen et al., 2005; Vendeville, 2005) which results either from gravity gliding or gravity spreading. Gravity spreading is the vertical collapse and spreading of a wedge under its own weight as opposed to gravity sliding which is defined as the downslope translation of a body. The key controls for gravity spreading are the dip of the upper surface, the friction along the detachment and the internal strength of the wedge of sliding material (Rowan et al., 2000). In the case of the MTD in our study area, at some point the mass transport body distorted under its own weight and the sediments started spreading out under the influence of gravity. This left an impression of “v” shaped scour marks that is observed in seismic and highlighted by strong k_2 anomalies (Figure 15).

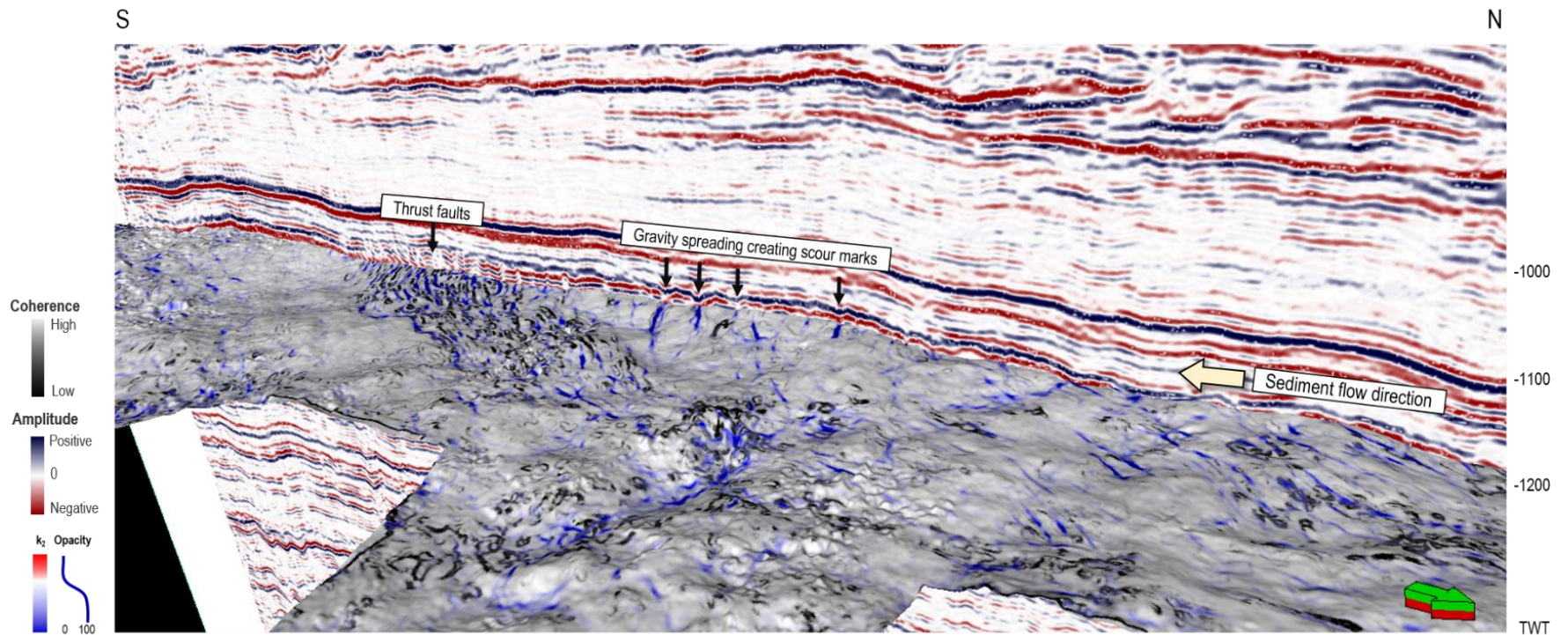


Figure 15: Top of MTD surface co-rendered with coherence and k2 anomalies highlighting the thrust faults and “v” shaped scour marks. Overall sediment direction is interpreted to be coming in from the North.

Although curvature and coherence are both useful in delineating faults, they are not redundant attributes but instead are complementary (Marfurt, 2018; Figure 14). In general, coherence, most positive-curvature, and most negative-curvature anomalies often do not align with each other (Marfurt, 2018). For the thrust faults within the MTD, low coherence anomalies are usually aligned along the fault trace, positive-curvature anomalies are shifted towards the hanging wall, and negative-curvature anomalies are shifted towards the footwall, thereby bracketing the fault trace. k_2 anomaly further highlights the scour marks that are left by the sediments due to gravity spreading.

Seismic Amplitude

Although not a geometric attribute, seismic amplitude is quick and easy way to look at stratigraphic features without involving strenuous attribute calculations. Seismic amplitude is a measure of rock layers that have contrasting impedance (product of density and velocity) values and can be positive, negative or zero depending on the relative impedance of the stratigraphic layer.

For a picked upper Leonard horizon, amplitudes values were extracted and viewed to understand the MTD geometry. Figure 10 illustrates how the amplitude anomalies map out going up the MTD stratigraphic section. The sinusoidal path taken by the sediments in the first MTD succession can be observed (Figure 16A) which highlights the translational regime of the mass movement. The imbricate thrust faults towards the compressional regime are hard to discern by studying amplitude anomalies by themselves. In general, impedance change can be inferred from the low and high amplitude anomalies but the plan

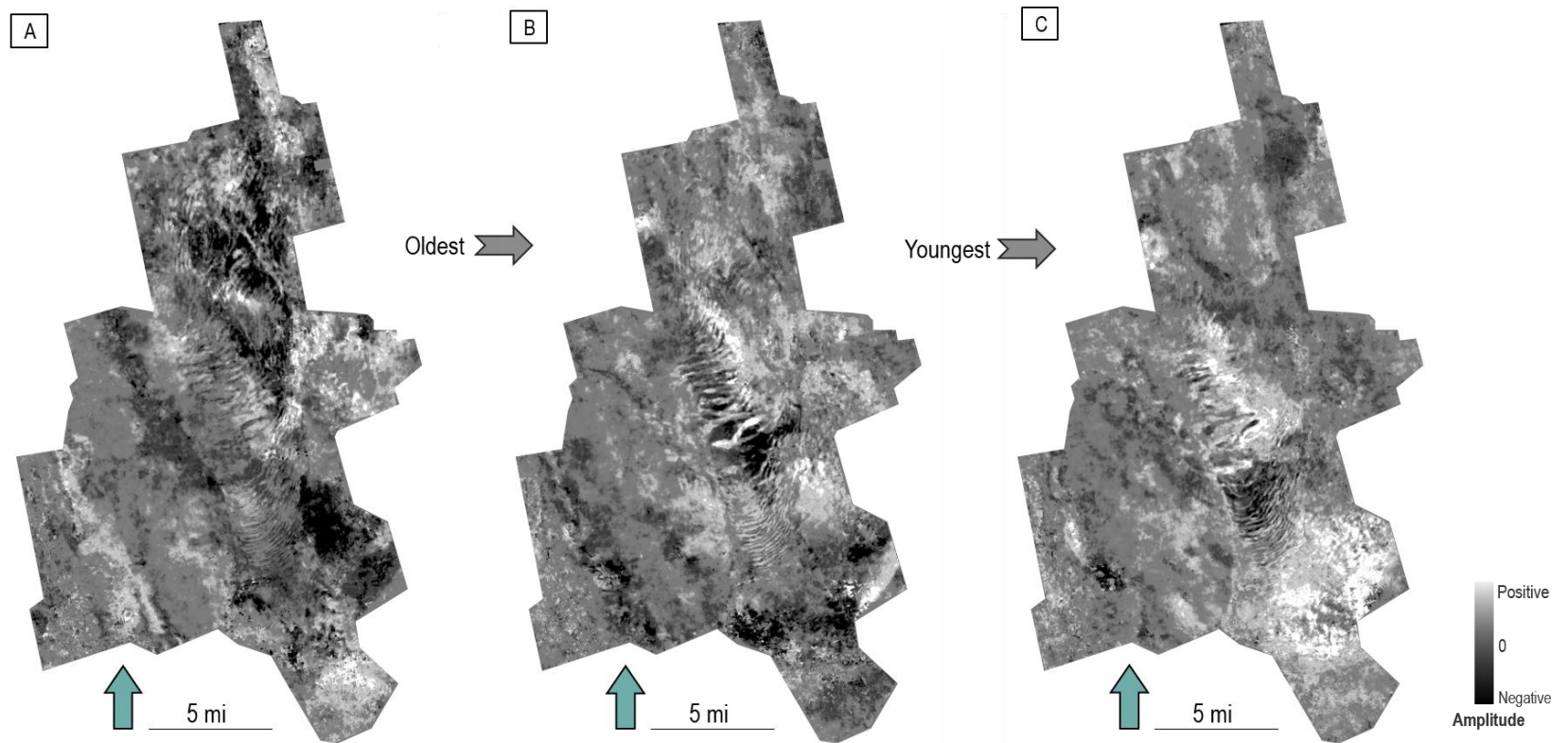


Figure 16: Seismic amplitude values extracted on stratal slice showing the change in amplitude anomalies going up the MTD stratigraphic section (left to right). The overall geometry of the MTD is hard to discern using amplitude values by itself

view does not help much in characterizing the external morphology of the MTD. Well logs has to be incorporated to make any lithology (impedance change) interpretations and understand the MTDs composition.

Lithologic character of the MTD in the Midland Basin

Mass movements have the potential to move vast amounts of sediment from shelf/slope to deep water settings and alter the original stratification and lithologic compositions. Such modifications can increase lithologic complexity and can be critical for hydrocarbon exploration. One way to understand the complexity within the MTD mapped in the study area is through the use of wireline logs. Besides their traditional use in exploration to assist with structure and isopach mapping, wireline logs help define physical rock properties such as lithology, porosity and permeability (Asquith et al., 1982) and aid in our understanding of the complexities within the rocks. As discussed by Posamentier (2007), it is imperative to integrate borehole data along with seismic section and plan view to properly define MTDs and understand their lithological character. Gamma ray and resistivity logs are used in this study to understand the lithologic character of the MTD.

Gamma-ray response correlates with increasing clay or organic matter and to a lesser extent with increasing feldspar owing to radioactive potassium (Hamlin et al., 2013). Carbonates exhibit the lowest gamma-ray response, while organic rich rocks including shales and laminated siltstones exhibit the highest gamma-ray response.

Resistivity logs are primarily used to identify hydrocarbon versus water bearing zones and indicate permeable zones (Asquith et al., 1982). However, they can be used for lithofacies identification where high resistivity typically corresponds to carbonates or tightly cemented sandstones with low clay content and permeability. Organic matter also increases resistivity. Laminated siltstones and permeable rocks usually exhibit low resistivity response.

Asmus and others (2013) gives us an insight on the MTDs response on image logs and conventional logs in the Upper Bone Spring formation (Upper Leonard) of the Delaware basin. According to the study, direct correlation of cores to image logs reveal that MTDs can be identified directly from image logs resulting in contrasting resistivity patterns. The study correlated a sharp decrease in gamma-ray response for these deposits, indicating an increase in limestone. For the same gamma-ray response, resistivity logs exhibited a sharp increase which corresponds to moderate to high resistivity (skeletal-rich) response on image logs.

In the study area, 3 wells were analyzed using gamma-ray and resistivity logs to understand the lithologic character of the MTD. Figure 17 shows a cross section highlighting wells X and Y that covers the compressional regime of the MTD and well Z which is located outside the MTD. The well outside the MTD gives us the lithologic composition of the upper Leonard sea floor on which the MTD deposition occurred. The logs were hung on the upper Spraberry formation and the top and base of MTD was picked

on low gamma-ray/high resistivity beds. The MTD interval in the study area is 350 feet thick.

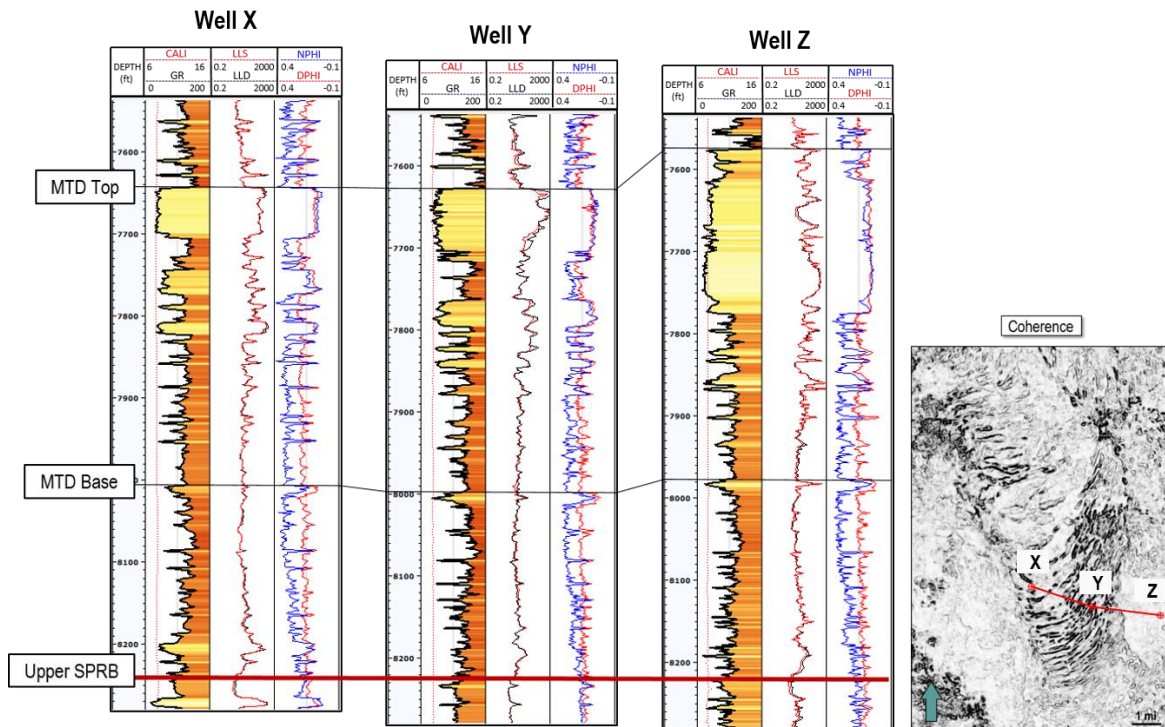


Figure 17: Well logs indicating MTD as a mix of carbonates and siliciclastic sediments.

Based on the density value of 2.63 g/cc, the low gamma-ray package indicates limestone (calcareous lithofacies) whereas a high gamma-ray response is interpreted as shales (siliciclastic lithofacies). Hence, well X and Y indicate a mix of calcareous and siliciclastic sediments and makes up the lithologic composition for the MTD. The porosity logs provide additional information about rock properties. Calcareous rocks typically have higher densities and faster sonic travel time than siliciclastic sediments. A large separation between the density and neutron porosity curves indicate clay rich rocks and low separation

indicates a tighter rock with less porosity. Well Z shows a higher concentration of calcareous sediments within the MTD interval with low gamma-ray/high resistivity response which are interpreted as the slope carbonates of the Central Basin Platform. With the help of seismic attributes along with well log analysis, the overall interpretation of the MTD is discussed in the next section.

CHAPTER VI

DISCUSSION AND CONCLUSIONS

Mass transport deposits (MTDs) observed in the Permian Basin are widespread deposits and can extend up to several miles. Posamentier (2006) estimates that up to 50% of the entire section can be moved during these processes. However, this estimate may be low as seismic resolution may be unable to detect finer scale mass movement processes. The upper Leonard MTD was interpreted throughout the 440 mi² Fasken C Ranch seismic survey in the Midland basin. This allowed observations of how sedimentary features flow during mass transports and the resulting sediment deposition.

The MTD mapped in the study area covers the translational and compressional regime of the mass movement. Kinematic evidence provided by the upper Spraberry structure suggests the MTD flow direction was from the North toward bathyal depths as the sediments follow the peak and saddle morphology of the Horseshoe Atoll. Seismic attributes (Figure 18) delineated the structural morphology of the sedimentary flow and helped compartmentalize the MTD (lateral wall, thrust faults, lobate shape and gravity spreading). The interpreted lobate shape of the MTD is due to the shearing of the sediments as they are restricted by the presence of the lateral wall. The slumping comes to a stop where the flow encounters an upper Leonard high towards the compressional regime and as the structure starts climbing up towards the west on the Central Basin Platform.

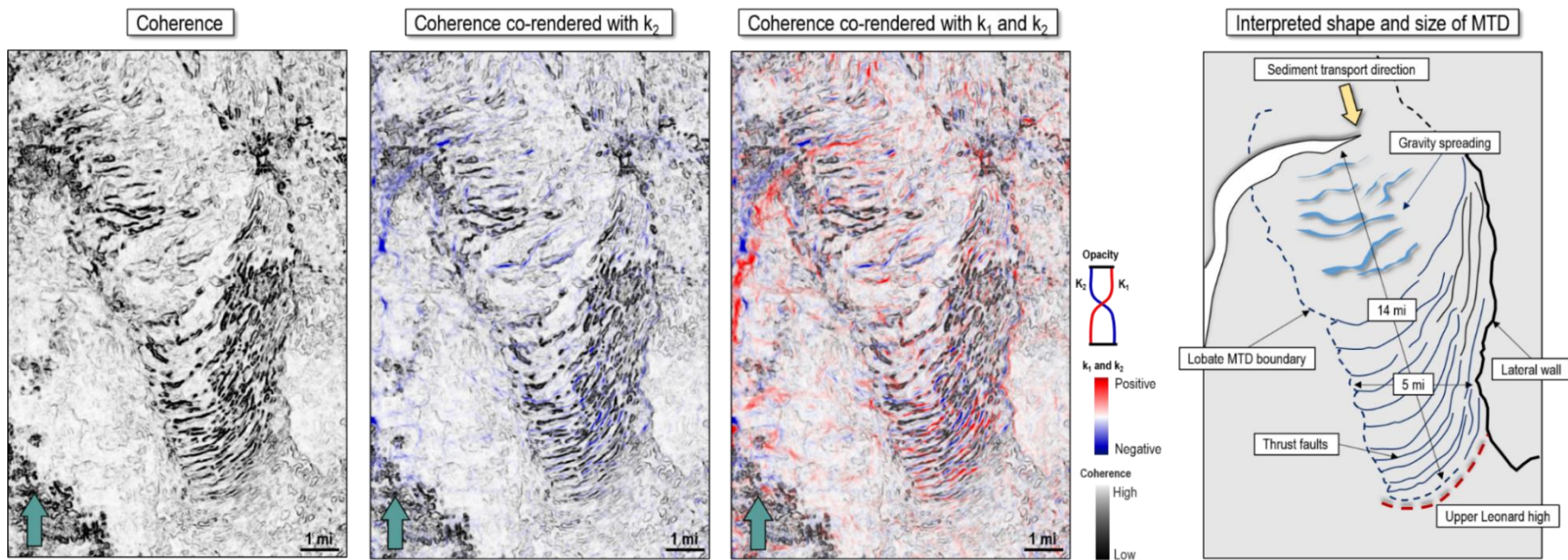


Figure 18: Overall interpretation of the Upper Leonard MTD observed in the Midland basin.

Three driving forces possibly responsible for the origin of the compressional structures are gravity, compressional stress resulting from rear-push and shear stress resulting from friction. The k_2 anomaly that highlights the footwall of the thrust faults is the same k_2 anomaly that highlights the “v” shaped scour marks at the upper MTD body due to gravity spreading. The curved “arm” (highlighted by strong k_1 and k_2 anomaly) coming off the Central Basin Platform is interpreted as a bend in the structure that is affected by a deep seated Paleozoic fault and may have acted as a constraint on the internal kinematics of the MTD and how the sediments were getting deposited.

The 350 feet thick MTD lithology is composed of carbonates and shales with moderate to high resistivity response and agrees with wireline correlations of the cyclic Leonardian platform deposits prograding towards the basin from clinoformal carbonates into flat lying calcareous and siliciclastic intervals (Ruppel et al., 2000; Asmus et al., 2013). A study conducted in the Delaware Basin demonstrated that MTDs can enhance production if targeted optimally where the faults enhance production rather than restrict it (Allen, 2013). This study investigated that the first well drilled inside the MTD zone of the 2nd Bone Spring sand had a 30 day average IP of 835 BOPD, which greatly outperformed the average 2nd Bone Spring well of 344 BOPD located locally but outside the MTD. Based on wireline correlations and their location in the depositional system, the reservoir potential for the MTD looks promising in the Midland Basin.

REFERENCES

Al-Dossary, S., and Marfurt K. J., (2006). 3D volumetric multispectral estimates of reflector curvature and rotation, *Geophysics*, 71, no. 5, P41-P51.
<https://doi.org/10.1190/1.2242449>

Allen, J., Schwartz, K., DeSantis, J., Koglin, D., and Chen, F., (2013). Integration of Structure and Stratigraphy in Bone Spring Tight Oil Sandstones using 3D Seismic in the Delaware Basin, TX. Unconventional Resources Technology Conference.

Amerman, R., (2009). Deepwater mass-transport deposits: Structure, Stratigraphy, and Implications for Basin Evolution.

Anderson, L.T., Hansen, D.L. and Huuse, M., (2005). Numerical modelling of thrust structures in unconsolidated sediments: implications for Glaciotectonic deformation. *J. Struct. Geol.*, 27, 587–596

Asmus, J. J., and Grammer G. M., (2013). Characterization of deepwater carbonate turbidites and mass-transport deposits utilizing high-resolution electrical borehole image logs: Upper Leonardian (Lower Permian) Upper Bone Spring Limestone, Delaware Basin, Southeast New Mexico and West Texas: *Gulf Coast Association of Geological Societies Transactions*, v. 63, p. 27–65.

Asquith, G., and Gibson, C., (1982). *Basic Well Log Analysis for Geologists*. The American Association of Petroleum Geologists.

Bakken, B., (1987). Sedimentology and syndepositional deformation of the Ross Slide, Western Irish Namurian Basin, Ireland. Unpublished Cand. Scient. Thesis: Geological Institute, Dep. A, University of Bergen, Bergen, Norway, XXX p.

Bhatnagar, P., M. Scipione, S. Verma, and R. Bianco, 2018, Characterization of mass transport deposit using seismic attributes: Spraberry Formation, Midland Basin, West Texas: *SEG Technical Program Expanded Abstracts*, 1618-1622.
<https://library.seg.org/doi/abs/10.1190/segam2018-2998610.1>

Bhatnagar, P., C. Bennett, R. Khoudaiberdiev, S. Leopard, and S. Verma, 2017, Seismic attribute illumination of a synthetic transfer zone: *SEG Technical Program Expanded Abstracts*, pp. 2112-2116. <https://doi.org/10.1190/segam2017-17664850.1>

Bull, S., Cartwright, J., and Huuse, M., (2009). A review of kinematic indicators from mass transport complexes using 3D seismic data. *Marine and Petroleum Geology*, 26(7), 1132–1151.

Butler, R., Sanchez A.D.P., McCaffrey B., Eggenhuisen J., Haughton P., Barker S., Hakes B., and Apps G., (2006). Dynamic formation of Rugosity on Mass Transport Complexes – Implications for Emplacement Dynamics , SEPM Research Symposium: The Significance of Mass Transport Deposits in Deepwater Environments II, AAPG Annual Convention, April 9-12, 2006 Technical Program.

Carpenter, G., (1987). The relation of clathrates and sediment stability, in Conference on Continental Margin Mass Wasting and Pleistocene Sea-Level Changes, August 13–15, 1980: U.S. Geological Survey, Circular, p. 88–95

Davies, R.J., Posamentier, H.W., Cartwright, J.A. and Wood, L., (2007). Seismic geomorphology: Applications to Hydrocarbon Exploration and Production. *Geologic Society, London, Special Publications*, 277.

Dingle, R.V., (1977). The anatomy of a large submarine slump on a sheared continental margin (SE Africa): *Geological Society of London, Journal*, v. 134, p. 293–310.

Festa A., Ogata K., Pini G.A., and Dilek Y., (2016). Origin and Significance of Olistostromes in the Evolution of Orogenic Belts: A Global Synthesis. *Gondwana Research* 39:180-203. DOI: 10.1016/j.gr.2016.08.002

Gawloski, T. F., (1987). Nature, distribution, and petroleum potential of Bone Spring detrital sediments along the Northwest Shelf of the Delaware Basin, in D. Cromwell and L. Mazzullo, eds, *The Leonardian facies in West Texas and Southeast New Mexico and guidebook to the Glass Mountains, West Texas: Permian Basin Section of the Society of Economic Paleontologists and Mineralogists Publication 87–27*, Midland, Texas, p. 85–106.

Hamlin, H.S., and Baumgardner R. W., (2013). Wolfberry (Wolfcampian-Leonardian) Deep-Water Depositional Systems in the Midland Basin: Stratigraphy, Lithofacies, Reservoirs, and Source Rocks.

Handford, C. R., (1981a). Deep-water facies of the Spraberry Formation (Permian), Reagan County, Texas, in Siemers, C. T., Tillman, R. W., and Williamson, C. R., eds., *Deep- water clastic sediments-a core workshop: Society of Economic Paleontologists and Mineralogists Core Workshop NO. 2*, p. 372-395.

Handford, C. R., (1981b). Sedimentology and genetic stratigraphy of Dean and Spraberry Formations (Permian), Midland Basin, Texas: American Association of Petroleum Geologists Bulletin, v. 65, no. 9, 1602-1 61 6.

Hills, J.M., (1983). Sedimentation, tectonism, and hydrocarbon generation in Delaware Basin, West Texas and Southeastern New Mexico. Web.

Hoak, T.; Sundberg, K. and Ortoleva, P., (1998). Overview of the Structural Geology and Tectonics of the Central Basin Platform, Delaware Basin, and Midland Basin, West Texas and New Mexico. December 31, 1998.

Khoudaiberdiev, R., C. Bennett, P. Bhatnagar, and S. Verma, 2017, Seismic interpretation of Cree Sand channels on the Scotian Shelf: SEG Technical Program Expanded Abstracts, pp. 2008-2012. <https://doi.org/10.1190/segam2017-17742372.1>

Jenner, K.A., Piper, D.J.W., Campbell, D.C., and Mosher, D.C., (2007). Lithofacies and origin of late Quaternary mass transport deposits in submarine canyons, central Scotian Slope, Canada: Sedimentology, v.54, p. 19–38.

Leeder, M.R., (1987). Sediment deformation structures and the palaeotectonic analysis of sedimentary basins, with a case study from the Carboniferous of northern England, in Jones, M.E., and Preston, R.M.F., eds., Deformation of Sediments and Sedimentary Rocks: Geological Society of London, Special Publication 29, p. 137–146.

Lewis, K.B., (1971). Slumping on continental slope inclined at 1–4°: Sedimentology, v. 16, p. 97-110.

Luo, Y., Higgs W. G., and Kowalik W. S., (1996). Edge detection and stratigraphic analysis using 3-D seismic data: 66th Annual International Meeting, SEG, Expanded Abstracts, 324–327.

Marfurt, K.J., (2018). Seismic Attributes as the Framework for Data Integration throughout the Oilfield Life Cycle. 2018 Distinguished Instructor Short Course. Society of Exploration Geophysicist.

Martinsen, O.J., and Bakken, B., (1990). Extensional and compressional zones in slumps and slides in the Namurian of County Clare, Eire: Geological Society of London, Journal, v. 147, p. 153–164.

Martinsen, O.J., (1994). Mass movements, *in* Maltman, A., ed., The Geological Deformation of Sediments: London, Chapman & Hall, p. 127–165.

Martinez, F.J., (2010). 3D Seismic Interpretation of Mass Transport Deposits: Implications for Basin Analysis and Geohazard Evaluation. *Advances in Natural and Technological Hazards Research*, Vol 28.

Maslin, M., Mikkelsen, N., Vilela, C., and Haq, B., (1998). Sea-level- and gas-hydrate-controlled catastrophic sediment failures of the Amazon Fan: *Geology*, v. 26, p. 1107–1110.

Moscardelli, L., Wood, L., and Mann, P., (2006). Mass-transport complexes and associated processes in the offshore area of Trinidad and Venezuela: *American Association of Petroleum Geologists, Bulletin*, v. 90, p.1059–1088.

Nemec, W., (1991). Aspects of sediment movement on steep delta slopes, in Colella, A., and Prior, D.B., eds., *Coarse-Grained Deltas: International Association of Sedimentologists, Special Publication 10*, p. 29–73.

Nissen, S.E., Haskell, N.L., Steiner, C.T., and Cotterill, K.L., (1999). Debris flow outrunner blocks, glide tracks, and pressure ridges identified on the Nigerian continental slope using 3-D seismic coherency. *The Leading Edge*, 18(5), 595-599.

Playton, T. E., and Kerans C., (2002). Slope and toe-of-slope deposits shed from a late Wolfcampian tectonically active carbonate ramp margin: *Gulf Coast Association of Geological Societies Transactions*, v. 52, p. 811–820

Posamentier H.W., and Martinsen O.J., (2010). The Character and Genesis of Submarine Mass-Transport Deposits: Insights from Outcrop 3D Seismic Data. *SEPM Special Publication No. 95*.

Posamentier H.W., (2017). *Seismic Stratigraphy and Geomorphology – The Next Frontier 21st Century Reservoir Characterization*. American Association of Petroleum Geologists (AAPG) South West Section (SWS) Bill Hailey short course.

Posamentier, H.W., and Walker, R.G., (2006). Deep-water turbidites and submarine fans, in Posamentier, H.W., and Walker, R.G., eds., *Facies Models Revisited: SEPM, Special Publication 84*, p. 397–520

Posamentier, H.W., Meizarwin, Wisman, P.S., and Plawman, T., (2000). Deep water depositional systems—ultra-deep Makassar Strait, Indonesia, in Weimer, P., Slatt, R.M, Coleman, J., Rosen, N.C., Nelson, H., Bouma, A.H., Styzen, M.J., and Lawrence, D.T., eds., *DeepWater Reservoirs of the World: Gulf Coast Section SEPM Foundation, 20th Annual Bob F. Perkins Research Conference*, p. 806–816

Posamentier H.W., and Kolla V., (2003). Seismic geomorphology and stratigraphy of depositional elements in deep-water settings. *J Sed Res* 73:367–388.

Prior, D.B., and Coleman, J.M., (1979). Submarine landslides: geometry and nomenclature: *Zeitschrift für Geomorphologie*, v. 23, p. 415–426.

Qi, J., Li, F., and Marfurt, K.J., (2017). Multiazimuth coherence, *Geophysics*, 82, no.6, O83-O89. <https://doi.org/10.1190/geo2017-0196.1>

Rapier, R., (2018). What Record Oil Production In The Permian Basin Looks Like. *Forbes*, Forbes Magazine, 15 Jan. 2018, www.forbes.com/sites/rpapier/2018/01/15/record-oil-production-in-the-permian-basin/#5d9fb21e4497.

Rowan, M.G., Peel, F.J. & Vendeville, B.C., (2004). Gravity driven fold belts on passive margins. In: *Thrust Tectonics and Hydrocarbon Systems* (Ed. by McClay K.R.), AAPG Memoir, 82, 157–182.

Ross, C. A., (1986). Paleozoic evolution of the southern margin of the Permian Basin: *Geological Society of America Bulletin*, v. 97, p. 536–554.

Ruppel, S. C., Ward, W. B., Ariza, E. E., and Jennings, J. W., Jr., (2000). Cycle and sequence stratigraphy of Clear Fork reservoir-equivalent outcrops: Victorio Peak Formation, Sierra Diablo, Texas, in Lindsay, R. F., Ward, R. F., Trentham, R. C., and Smith, A. H., eds., *Classic Permian geology of West Texas and southeastern New Mexico; 75 years of Permian Basin oil & gas exploration and development: West Texas Geological Society Publication No. 00-108*, p. 109–130.

Saller, A. H., J. W. Barton, and Barton R. E., (1989). Slope sedimentation associated with a vertically building shelf, Bone Spring Formation, Mescalero Escarpe Field, southeastern New Mexico, in P. D. Crevello, J. L. Wilson, F. Sarg, and J. F. Read, eds., *Controls on carbonate platform and basin development: Society of Economic Paleontologists and Mineralogists (Society for Sedimentary Geology) Special Publication 44*, Tulsa, Oklahoma, p. 275– 288.

Seed, H.B., (1968). Landslides during earthquakes due to soil liquefaction: *American Society of Civil Engineers, Proceedings, Journal of Soil Mechanics Foundation*, v. 94, p. 1055–1122.

Shipp R.C., Weimer P., Posamentier H.W., (2011). Mass-Transport Deposits in Deepwater Settings: An Introduction. <https://doi.org/10.2110/sepmsp.096.003>.

Trentham, R., (2018). Donated to The University of Texas of the Permian Basin. Modified and used with permission.

Tyler, N., Gholston, J. C., and Guevara, E. H., (1997). Basin morphological controls on submarine-fan depositional trends: Spraberry Sandstone, Permian Basin, Texas: University of Texas at Austin Bureau of Economic Geology Geological Circular 97-6, 43 p.

Vendeville, B.C., (2005). Salt tectonics driven by sediment progradation: part i-mechanics and kinematics. *Am. Assoc. Pet. Geol. Bull.*, 89, 1071–1079

Vest, E. L., (1970). Oil fields of Pennsylvanian-Permian Horseshoe Atoll, West Texas, in *Geology of giant petroleum fields: American Association of Petroleum Geologists Memoir 14*, p. 185–203.

Verma, S., S. Bhattacharya, B. Lujan, D. Agrawal, S. Mallick, 2018, Delineation of early Jurassic aged sand dunes and paleo-wind direction in southwestern Wyoming using seismic attributes, inversion, and petrophysical modeling: *Journal of Natural Gas Science and Engineering*, 60, 1-10. <https://doi.org/10.1016/j.jngse.2018.09.022>.

Wiggins, W. D., and Harris P. M., (1985). Burial diagenetic sequence in deep-water allochthonous dolomites: Permian Bone Spring Formation, Southeast New Mexico: *Society of Economic Paleontologists and Mineralogists (Society for Sedimentary Geology) Core Workshop 6*, Tulsa, Oklahoma, p. 140–173.